Bioorganic Chemistry 87 (2019) 821–837

Contents lists available at ScienceDirect

Bioorganic Chemistry

journal homepage: www.elsevier.com/locate/bioorg

Synthesis and biological evaluation of purine-pyrazole hybrids incorporating thiazole, thiazolidinone or rhodanine moiety as 15-LOX inhibitors endowed with anticancer and antioxidant potential

Ola S. Afifi[a], Omaima G. Shaaban[a,b,*], Heba A. Abd El Razik[a], Shams El-Dine A. Shams El-Dine[a], Fawzia A. Ashour[a], Alaa A. El-Tombary[a], Marwa M. Abu-Serie[c]

[a] Department of Pharmaceutical Chemistry, Faculty of Pharmacy, Alexandria University, Alexandria 21521, Egypt
[b] Department of Pharmaceutical Chemistry, Faculty of Pharmacy and Drug Manufacturing, Pharos University in Alexandria, Alexandria, Egypt
[c] Genetic Engineering and Biotechnology Research Institute (GEBRI), City of Scientific Research and Technological Applications (SRTA-City), Alexandria, Egypt

ABSTRACT

Novel purine-pyrazole hybrids combining thiazoles, thiazolidinones and rhodanines, were designed and tested as 15-LOX inhibitors, potential anticancer and antioxidant agents. All tested compounds were found to be potent 15-LOX inhibitors with IC_{50} ranging from 1.76 to 6.12 μM. The prepared compounds were evaluated *in vitro* against five cancer cell lines: A549 (lung), Caco-2 (colon), PC3 (prostate), MCF-7 (breast) and HepG-2 (liver). Compounds **7b** and **8b** displayed broad spectrum anticancer activity against the five tested cell lines (IC_{50} = 18.5–95.39 μM). While, compound **7h** demonstrated moderate anticancer activity against lung A549 and colon Caco-2 cell lines. Antioxidant screening revealed that six compounds (**5a, 5b, 6b, 7b, 7h** and **8b**) with IC_{50} ranging from 0.93 to 14.43 μg/ml were found to be more potent scavengers of 2,2- diphenyl-1-picrylhydrazyl (DPPH) than the reference ascorbic acid with IC_{50} value of 15.34 μg/ml. Compounds **7b, 7h** and **8b,** when evaluated for their antioxidant activity, where found to be potent DPPH scavengers. Moreover, compound **7b** displayed twice the potency of ascorbic acid as NO scavenger. Docking study was performed to elucidate the possible binding mode of the most active compounds with the active site of 15-LOX enzyme. Collectively, the purine-pyrazole hybrids having thiazoline or thizolidinone moieties (**7b, 7h** and **8b)** constitute a promising scaffold in designing more potent 15-LOX inhibitors with anticancer and antioxidant potential.

1. Introduction

The increasing spread of malignant tumors had stimulated the subsequent increase in designing various anticancer agents possessing different mechanisms of action.

Lipoxygenase (LOX) pathway is important for producing hydroxyeicosatetraenoic acids (HETEs) or leukotrienes (LTs) from arachidonic acid (AA). Isoenzymes of LOX include 5-LOX, 12-LOX, and two 15-LOX isoforms [1].

The role of 15-LOX metabolites has been reported in development of many cancer cell lines such as breast and prostate [2,3]. In breast cancer they promoted the invasion of tumor cells into lymphatic vessels and production of lymph node metastasis [2]. In prostate cancer, linoleic acid is converted into 13-S-hydroxyoctadecadienoic acid (13-(S)-HODE) and other metabolites which alter cellular signaling pathways and therefore inappropriate expression might change biological events and lead to tumor development [4]. 15-LOX over-expression showed an increase in the frequency of tumor formation, tumor size and angiogenesis, suggesting a growth promoting role for 15-LOX in the prostate cancer [5]. Based on the role of 15-LOX in promoting cancer, it could be claimed that 15-LOX inhibitors will be considered suitable as chemotherapeutic agents in the near future.

High levels of free radicals “oxidative stress” has been linked with cancer promotion and progression. Oxidative stress can cause uncontrolled proliferation and resistance to apoptosis through DNA mutation [6]. Damage of DNA by free radicals has been generally known as a main cause of cancer [7]. Therefore, preventing formation of free-radical and its consequent oxidative damage which can be accomplished by antioxidants and/or free-radical scavengers may be an essential therapeutic strategy in cancer treatment.

Thiazoles, thiazolidinones and rhodanines occupied unique position in the design and synthesis of anticancer [8–10] and antioxidant agents [11–13]. 5-Benzylidene-3-ethyl rhodanine (BTR-1) (**A**) (Fig. 1), induced a block at S phase of the cell cycle leading to apoptosis and hence it had cytotoxic effect on human leukemic cells [8]. A thiazole containing drug, tiazofurin (**B**) (Fig. 1), was found to have marked antitumor activity against P388 and L1210 leukemias and the Lewis lung carcinoma [9]. Moreover, 3-(4-bromophenyl)-2-[4-(dimethylamino)phenyl]thiazolidin-4-one (**C**) (Fig. 1), displayed considerable cytotoxicity against Reh and Nalm6 leukemic cells [10].

* Corresponding author.
E-mail address: omaima.Shaaban@pua.edu.eg (O.G. Shaaban).

https://doi.org/10.1016/j.bioorg.2019.03.076
Received 3 January 2019; Accepted 31 March 2019
Available online 01 April 2019

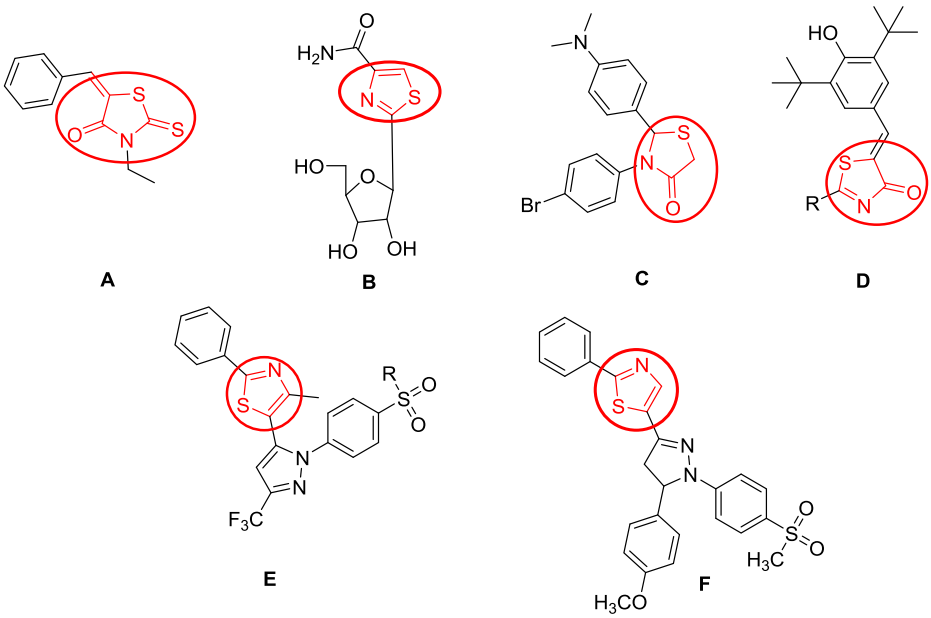

Fig. 1. Examples of structural leads possessing promising anticancer and/or 15-LOX inhibitory activity.

In addition, darbufelone and CI-987 (**D**) were reported as dual COX/LOX inhibitors (14) (Fig. 1). Abdelall et al. [14] reported the thiazolo/celecoxib analogues (**E**) and (**F**) (Fig. 1) as more potent 15-LOX inhibitors than meclofenamate sodium with IC_{50} values of 3.98–5.41 μM.

Purines constitute important scaffold in drug discovery as they are constituents of many bioactive heterocyclic compounds with diverse biological activities such as anticancer, antiviral, antimicrobial, anti-inflammatory, anticonvulsant, antimalarial and bronchodilator [15–21]. Purines were the first class of 15-LOX inhibitors to be reported in 2002 [22].

In addition, the purine-based compounds exhibit various mechanisms of anticancer activities such as inhibition of topoisomerase II [23], Hsp90 [24], CDK [25], PDK1 [26] or PDE [27]. Whereas, some purines are able to activate AMPK, 5′–adenosine monophosphate–activated protein kinase [28].

Our previous publication reported the synthesis, *in vitro* anticancer and antioxidant activities of several purines containing variously substituted pyrazoles [29], in which **I**, **II** and **III** exhibited promising anticancer and/or antioxidant activities (Fig. 2).

Enlightened by the aforementioned facts, it was designed to incorporate thiazole, thiazolidinone and rhodanine moieties as anticancer and 15-LOX inhibitor pharmacophores at the 4-position of the pyrazolyl purine scaffold either through one atom spacer as in compounds **4a-d** and **5a-d** or through three atom spacer as in compounds **7a-h** and **8a-h** (Fig. 3) aiming to obtain synergistic anticancer, antioxidant and 15-LOX inhibitory activity.

2. Results and discussion

2.1. Chemistry

The synthetic strategies adopted for the synthesis of the intermediate and target compounds are depicted in Schemes 1–3. The starting 7-ethyl-8-hydrazinyl-1,3-dimethyl-1*H*-purine-2,6(3*H*,7*H*)-dione **1**, **2a-d**, **3a-d** and **6a-h** were prepared following previously reported reaction conditions[29,30]. In Scheme 2, condensation of the pyrazolecarbaldehyde derivatives **3a-d** with 4-(4-oxo-2-thioxothiazolidin-3-yl)benzenesulfonamide in dry dioxane in presence of catalytic amount of piperidine according to knoevenagel condensation reaction conditions [31–33] afforded compounds **4a-d** in good yields. IR spectra of compounds **4a-d**

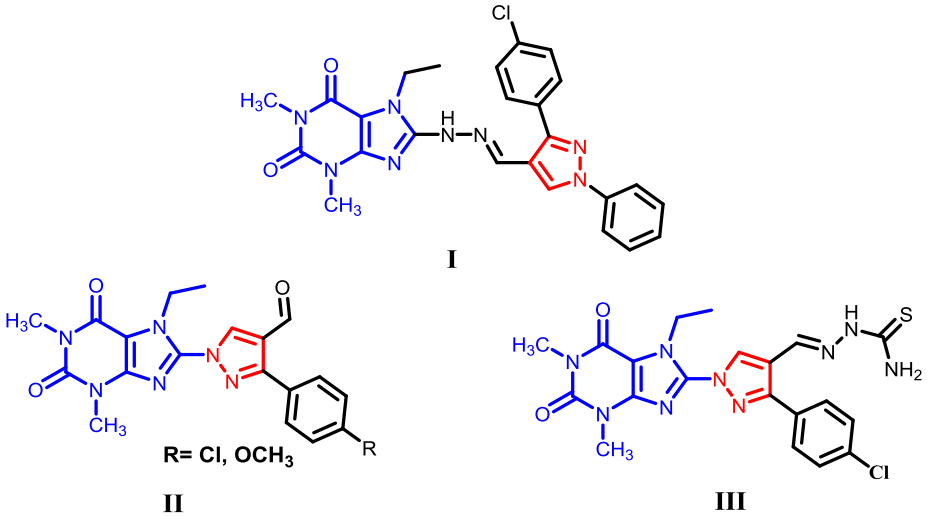

Fig. 2. Reported pyrazolyl purine derivatives with promising anticancer and/or antioxidant activities.

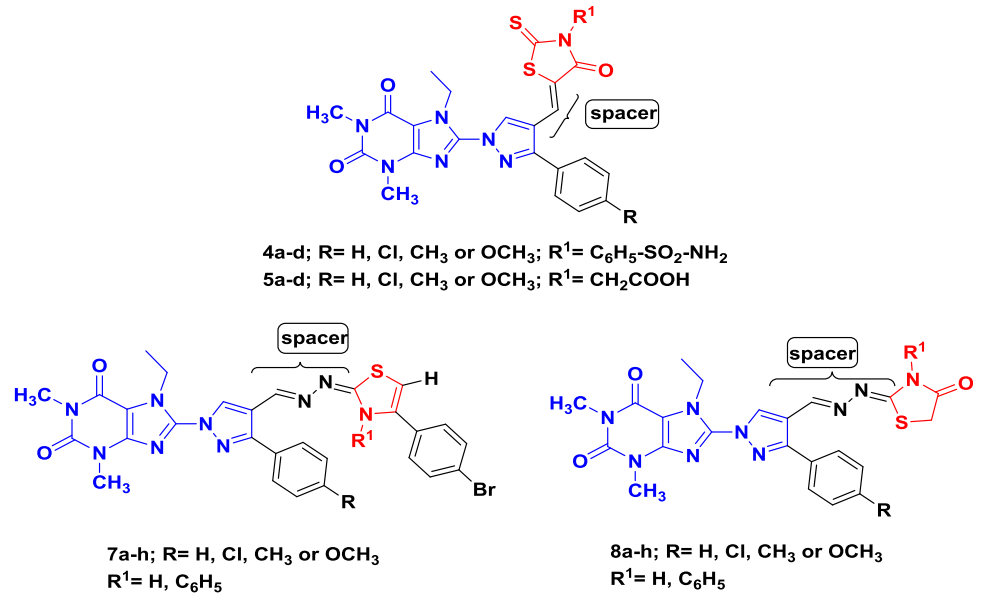

Fig. 3. Design of the target 15-LOX inhibitors, anticancer and antioxidants.

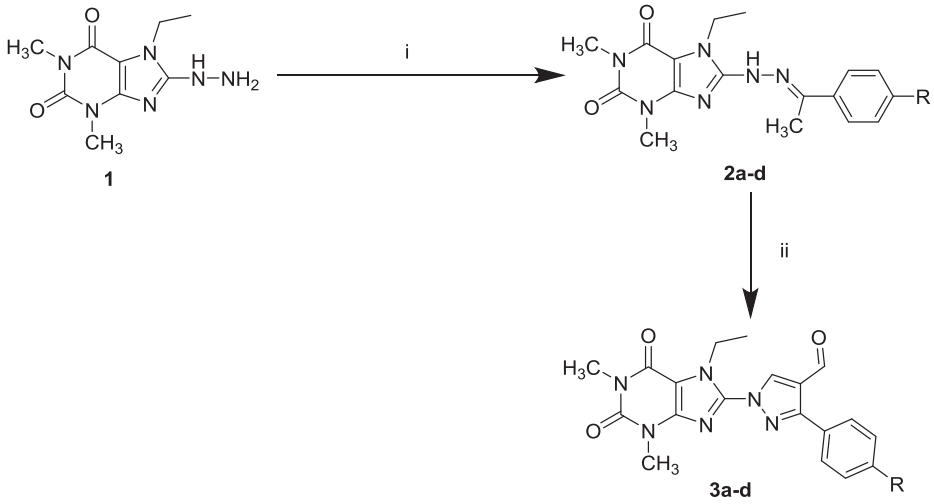

Scheme 1. Synthesis of compounds **1–3**.

showed the appearance of absorption bands at 3430–3218 cm^{-1} due to NH_2 group, at 1351–1346 cm^{-1} due to SO_2 group. The absorption bands due to C═O, C═N and C–S–C, beside C–O–C in compound **4d**, appeared at their expected frequencies. ^{1}H NMR spectra of compounds **4a-d** lacked the aldehydic proton in the precursor and showed the singlet at 8.63–8.75 ppm due to pyrazole-C_5-H in addition to signals due to C═CH and NH_2 protons appeared as two singlets at 7.61–7.63 ppm and 7.52–7.53 ppm, respectively in case of compounds **4c** and **4d** and were included within the multiplet due to aromatic protons at 7.49–7.72 ppm in case of compounds **4a** and **4b**. Signals due to other aliphatic and aromatic protons appeared at their expected chemical shifts. Heating the pyrazolecarbaldehyde derivatives **3a-d** with 2-(4-oxo-2-thioxothiazolidin-3-yl)acetic acid in dry dioxane in the presence of ammonium acetate gave compounds **5a-d** following knoevenagel condensation reaction conditions [31–33]. IR spectra of compounds **5a-d** showed the stretching absorption bands due to OH group at 3472–3439 cm^{-1}. In compound **5a**, the absorption band due to acid C═O function appeared at 1725 cm^{-1} whereas in compounds **5b-d**, a broad absorption bands due to the acid C═O function overlapping with the rhodanine –C═O and one of the purine C═O functions appeared at 1704–1659 cm^{-1}. In addition, the absorption bands due to the other purine C═O, C═N, C–S–C, besides C–O–C in compound **5d**, appeared at their expected frequencies. ^{1}H NMR spectra of compounds **5a-d** lacked the aldehydic proton in the precursor and showed a singlet at 4.48–4.68 ppm assigned for CH_2CO protons and singlets at 7.52–7.56 ppm due to C═CH in case of compounds **5b-d** while the signal due to C═CH proton in case of **5a** was included within the multiplet for phenyl-$C_{3,4,5}$-H at 7.56–7.58 ppm. The spectra also showed a singlet at 8.52–8.67 ppm due to pyrazole-C_5-H. The ^{1}H NMR spectrum of compound **5c** showed a deuterium exchangeable singlet due to OH group at 13.0 ppm. Signals due to other aliphatic and aromatic protons appeared at their expected chemical shifts.

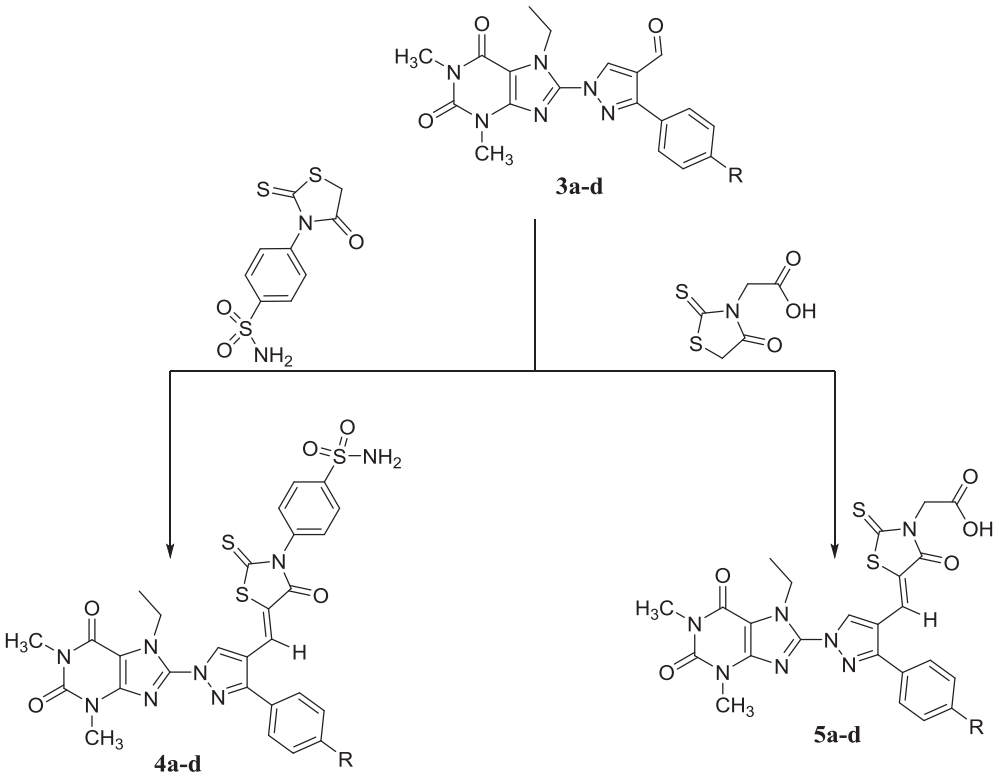

Scheme 2. Synthesis of compounds **4** and **5**.

Heating under reflux the pyrazolecarbaldehyde derivatives **3a-d** with the appropriate *N*-substituted thiosemicarbazide in dry dioxane in presence of catalytic amount of glacial acetic acid yielded the corresponding *N*-substituted thiosemicarbazones **6a-d** [30]. Compounds **7a-h** were prepared by treatment of the thiosemicarbazone derivatives **6a-h** with 4-bromophenacyl bromide in dry dioxane in the presence of anhydrous sodium acetate, adopting reported reaction conditions for preparation of analogous compounds [34]. IR spectra of compounds **7a-**

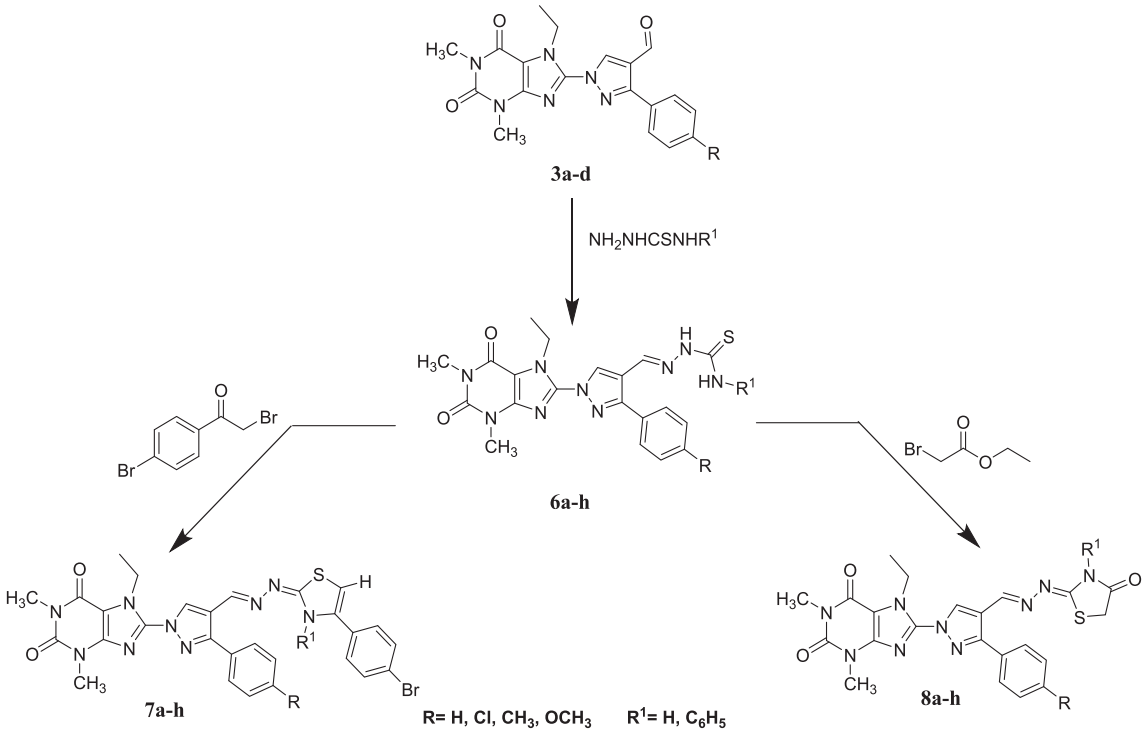

Scheme 3. Synthesis of compounds **7** and **8**.

h lacked the N—C═S absorption bands and showed absorption bands at 1296–1246 and 1084–1029 cm^{-1} assigned for C—S—C groups. In compounds **7a, 7c, 7e** and **7 g** (where R^1 = H), the spectra showed an absorption band at 3199–3221 cm^{-1} assigned for NH group. The spectra of **7a-h** also showed the absorption bands due to C═O and C═N functions, besides the C—O—C function in compounds **7g** and **7h**, appeared at their expected frequencies. ^{1}H NMR spectra of compounds **7a-h** showed three singlets at 6.45–7.34, 7.38–8.25 and 8.59–10.12 ppm assigned for thiazoline-C_5-H, pyrazole-C_5-H and N═CH protons, respectively. The spectra of compounds **7b, 7d, 7f** and **7h** (R^1 = C_6H_5) lacked the two deuterium exchangeable singlets due to 2 NH protons in the precursor while the spectra of compounds **7a, 7c, 7e** and **7g** (R^1 = H) showed a deuterium exchangeable singlet at 12.0–12.02 ppm due to NH proton. In addition, other signals due to aliphatic and aromatic protons appeared at their expected chemical shifts. Cyclization of thiosemicarbazones **6a-h** by heating with ethyl bromoacetate in dry dioxane in the presence of anhydrous sodium acetate following the reaction conditions adopted for the synthesis of analogous compounds [34] gave compounds **8a-h**. Their IR spectra lacked the N—C═S absorption bands and showed absorption bands at 1294–1239 and 1036–1029 cm^{-1} assigned for C—S—C groups. In compounds **8a, 8c, 8e** and **8 g** (where R^1 = H), the spectra showed an absorption band at 3442–3135 cm^{-1} attributed to the NH group. In addition, absorption bands due to C═O, C═N, besides C—O—C function in compounds **8g** and **8h** appeared at their expected frequencies. ^{1}H NMR spectra of compounds **8a-h** showed three singlets at 3.87–4.11, 8.34–8.50 and 8.70–8.84 ppm assigned for thiazolidinone-C_5-H, pyrazole-C_5-H and N═CH, respectively. Compounds **8a, 8c, 8e** and **8g** (where R^1 = H), showed a deuterium exchangeable singlet at 11.91–12.0 ppm due to the NH proton, while compounds **8b, 8d, 8f** and **8h**, lacked the two deuterium exchangeable singlets due to 2 NH protons in the precursor. Besides, other aliphatic and aromatic protons appeared at their expected chemical shifts.

2.2. Biological evaluation

2.2.1. In vitro 15-LOX inhibitory assay

Eighteen compounds were evaluated for their *in vitro* ability to inhibit 15-lipoxygenase enzyme, using Abnova 15-lipoxygenase inhibitor screening assay kit (catalog no. KA1329, Cayman Chemicals), according to the manufacturer's instructions. Meclofenamate sodium, quercetin and zileuton were used as a reference standard in this study. Lipoxygenase inhibitor screening assay kit detects and measures the hydroperoxides produced in the lipoxygenation reaction using a purified 15-LOX thus is considered a general detection method for lipoxygenase enzyme [35], and can be used to screen compounds which inhibit 15-LOX enzyme. The results were recorded in Table 1 as the compound's concentration causing 50% enzyme inhibition (IC_{50}) and they are the means of three determinations. Results revealed that all compounds (IC_{50} range 1.76–6.12 μM) exhibited potential 15-LOX inhibitory activity at concentration lower than that of the reference quercetin with IC_{50} = 6.87 μM. Seventeen tested compounds possess stronger LOX inhibitory activity (IC_{50} = 1.76–5.11 μM) than that of the standard inhibitor Meclofenamate sodium with IC_{50} = 5.64 μM. Compounds **4a**, **4b**, **5a**, **6b**, **7b**, **7d**, **7h**, **8b**, **8d** and **8h** (IC_{50} range 1.76–2.64 μM) showed potential 15-LOX inhibition activity at concentration lower than that of the standard inhibitor zileuton (IC_{50} = 3.98 μM). Among which, compounds **4a, 7d, 7h** and **8d** were the most potent (IC_{50} = 1.76–1.98 μM) demonstrating 2 times the potency of zileuton.

A deep insight on the structures of the test compounds revealed that the test pyrazole carboxaldehydes exerted moderate activity. Generally, condensation with rhodanine derivatives afforded compounds **4a**, **4b**, **4d**, **5a**, **5b** and **5d** with improved potency than the starting pyrazole carboxaldehydes. It is noted that the condensing products having acetic acid side chain (**5a**, **5b** and **5d**) showed better 15-LOX inhibitory activity than their benzene sulphonamide counterparts (**4a**, **4b** and **4d**). On the other hand, the thiosemicarbazone derivatives (**6b**, **6d** and **6h**) displayed improved efficacy than their pyrazole carboxaldehydes precursors. Moreover, cyclization of the thiosemicarbazone derivatives into thiazoline and thiazolidinone derivatives generally give rise to more potent inhibitors. Among which the thiazoline derivatives (**7b**, **7d** and **7h**) showed higher potency than the thiazolidinone counterparts (**8b**, **8d** and **8h**).

Table 1
Results of *in vitro* LOX.

Compound ID	IC_{50} (μM)*
3a	5.11
3b	4.62
3d	6.12
4a	1.96
4b	2.64
4d	3.14
5a	2.62
5b	3.42
5d	4.12
6b	2.81
6d	3.04
6h	4.19
7b	2.41
7d	1.76
7h	1.82
8b	2.33
8d	1.98
8h	2.55
Zileuton	3.98
Quercetin	6.87
Meclofenamate sodium	5.64

* Values are means of three determinations acquired using Abnova 15-lipoxygenase assay kit (catalog no. KA1329, Cayman Chemicals) and the deviation from the mean is < 10% of the mean value.

2.2.2. Anticancer screening

The newly synthesized compounds were screened for their potential anticancer activity against five human cancer cell lines, A549 (lung), Caco-2 (colon), PC3 (prostate), MCF-7 (breast) and HepG-2 (liver) cancer cell lines using 5-FU as a standard anticancer drug by using MTT assay, described by Mosmann [36].

The obtained data was represented in (Table 2) for the IC_{50} values of the tested compounds and 5-FU in μM. The results revealed that several compounds exhibited significant activity against all five tested cell lines. The most potent activity against A549 cell line was exhibited by compound **8b**. It was more potent than the reference drug 5-FU itself (IC_{50}: 18.85 and 83.03 μM, respectively), followed by compounds **7b** and **7h** with IC_{50} values 36.51 and 64.48 μM.

Moreover, compound **8b** showed pronounced anticancer activity against MCF-7 cell line comparable to 5-FU activity with IC_{50} value of 23.43 and 93.79 μM, respectively, while compound **7b** exhibited moderate activity with IC_{50} value 95.39 μM.

Similarly, compounds **7b** and **8b** exhibited potent activity to that produced by the standard drug against HepG-2 cell line (IC_{50}: 74.72, 23.08 and 96.86 μM, respectively).

In addition, higher cytotoxic potency than that of 5-FU against cancerous colon cell line Caco-2 was demonstrated by compound **8b** with IC_{50} value of 23.08 and 112.24 μM, respectively, while moderate activity with IC_{50} values of 94.25 and 109.28 μM was displayed by compounds **7b** and **7h**, respectively.

It is noteworthy that compound **8b** in addition to its high efficacy against A549, MCF-7, HepG-2 and Caco-2 cells, also displayed higher anticancer than 5-FU against prostate cancer cell line PC3 cell line (IC_{50}: 18.5, 82.26 μM, respectively). Furthermore, higher anticancer activity against PC3 cell line was observed by compound **7b** compared

Table 2
Anticancer activities (IC_{50} in μM) of the tested compounds on five human cancer cell lines.

Compound ID	IC_{50} (μM)* A549	IC_{50} (μM) MCF-7	IC_{50} (μM) HepG-2	IC_{50} (μM) Caco-2	IC_{50} (μM) PC3
3a	1431.06	3842.60	3650.20	3309.02	3494.54
3b	148.73	859.19	390.23	442.07	268.15
3d	953.21	1777.87	838.37	632.21	1060.70
4a	406.02	1595.86	1951.63	865.06	928.11
4b	3253.46	5320.12	4373.66	1992.59	1996.98
4d	481.17	341.65	331.78	486.77	824.30
5a	312.18	378.54	497.64	328.50	277.37
5b	572.15	664.97	449.80	642.62	496.72
5d	1831.78	1394.90	760.63	785.05	667.79
6b	396.32	235.97	276.54	708.30	497.92
6d	472.38	1373.54	1110.04	481.99	785.52
6h	369.24	761.97	522.93	469.85	532.07
7b	36.51	95.39	74.72	94.25	44.30
7d	436.67	801.42	524.79	854.05	891.70
7h	64.48	238.11	145.80	109.28	205.66
8b	18.85	23.43	23.08	23.08	18.50
8d	201.80	238.84	242.66	215.09	177.06
8h	170.84	261.02	277.09	360.75	283.11
5-FU	83.03	93.79	96.86	112.24	82.26

* Data were expressed as the means of two determinations ± SEM.

to the standard 5-FU, (IC_{50}: 44.30 and 82.26 μM, respectively).

It is worthy to point out that relative to the 5-FU with IC_{50} values between 82.26 and 112.24 μM against A549, MCF-7, HepG-2, Caco-2 and PC3 cell lines, compound **7b** possessed potential and broad spectrum anticancer activity with IC_{50} between 36.51 and 95.39 μM. Moreover, compound **8b** displayed broad spectrum anticancer activity with IC_{50} values ranging from 18.50 to 23.43 μM against all cell lines tested.

Structure activity correlations of the obtained results indicated that the pyrazole carboxaldehydes **3a**, **3b**, **3d**, and their rhodanine condensation products **4a**, **4b**, **4d**, **5a**, **5b** and **5d** didn't show pronounced anticancer activity. On the other hand, cyclization of the thiosemicarbazones **6a-h** afforded thiazolines **7b, 7d** and **7h** or thiazolidinones **8b, 8d** and **8h**. Among the thiazoline derivatives, compound **7b** possessed broad spectrum anticancer activity against all cell lines tested. While **7h** exhibited moderate activity against cancerous lung A-549 and colon Caco-2 cell lines. Among the thiazolidinone derivatives, compound **8b** displayed pronounced, broad spectrum anticancer activity than 5-FU against all cell lines tested.

2.2.3. Antioxidant screening

2.2.3.1. Determination of the free radical scavenging activity by the 1,1-diphenyl-2-picrylhydrazyl (DPPH) antioxidant screening assay method. This method measures the ability of the test compounds to scavenge free radicals against DPPH which produce a violet color in methanol at λ = 517 nm. An antioxidant could donate an electron that reduce DPPH and decay the violet color. The absorbance change recorded at λ = 517 nm is expressed as % inhibition of DPPH relative to the reference ascorbic acid. This method provides information on the ability of a compound to donate a hydrogen atom and thus showed the possible antioxidant efficacy. Scavenging activities were measured via the procedure followed by Braca et al. [37].

The antioxidant screening results (Table 3) revealed that all the tested compounds displayed variable antioxidant activity against DPPH with respect to ascorbic acid. The results indicated that compound **8b** demonstrated strong antioxidant activity against the DPPH radicals with IC_{50} of 0.93 μg/ml, relative to ascorbic acid having IC_{50} value of 15.34 μg/ml. Hence, compound **8b** can be considered as the best antioxidant among the tested compounds. In addition, compounds **5a, 5b, 6b, 7b** and **7h** exhibited good DPPH free radical scavenging potential with IC_{50} ranging from 4.89 to 14.43 μg/ml higher than that of the standard ascorbic acid with IC_{50} value of 15.34 μg/ml. Compounds **3b, 5d, 6d, 8d** and **8h** showed moderate antioxidant activity with IC_{50} values ranging from 15.93 to 29.25 μg/ml, respectively. The remaining compounds exhibited weak activity with IC_{50} ranging from 42.98 to 359.17 μg/ml.

Table 3
Results of *in vitro* antioxidant assay using DPPH.

Compound ID	IC_{50} (μg/ml)*
3a	231.47 ± 1.28
3b	19.67 ± 0.41
3d	56.99 ± 0.85
4a	56.2 ± 0.44
4b	359.17 ± 20.9
4d	187.75 ± 4.54
5a	6.18 ± 0.04
5b	14.43 ± 0.45
5d	29.25 ± 0.1
6b	10.24 ± 0.04
6d	28.74 ± 0.17
6h	42.98 ± 2.82
7b	5.71 ± 0.1
7d	53.51 ± 1.64
7h	4.89 ± 0.02
8b	0.93 ± 0.01
8d	15.93 ± 0.29
8h	26.9 ± 0.2
Ascorbic acid	15.34 ± 0.19

* Data were expressed as the means of two determinations ± SEM.

2.2.3.2. Determination of nitric oxide radical scavenging activity. Investigation of the potential of the tested compounds to scavenge nitric oxide (NO) free radical was determined via the method reported by Ho *et al.* [38]. This method depends on the production of nitric oxide from sodium nitroprusside solution at physiological pH that reacts with oxygen to give nitrite ions that can be determined by using Griess reagent.

The results listed in (Table 4) revealed that compounds **3b, 5b** and **7b** are stronger antioxidants with IC_{50} values of 30.46, 30.67 and 21.31 μg/ml, respectively, than the standard ascorbic acid with IC_{50} value of 45.64 μg/ml. Compounds **3d, 4d** and **5a** were nearly equipotent to the standard ascorbic acid with IC_{50} values of 43.66, 44.16 and 46.92 μg/ml, respectively.

Table 4
Results of *in vitro* antioxidant assay using NO.

Compound ID	IC_{50} (μg/ml)*
3a	109.68 ± 0.005
3b	30.46 ± 0.11
3d	43.66 ± 0.08
4a	60.87 ± 0.03
4b	74.14 ± 0.02
4d	44.16 ± 0.1
5a	46.92 ± 0.09
5b	30.67 ± 0.11
5d	84.52 ± 0.09
6b	72.54 ± 0.11
6d	98.71 ± 0.005
6h	118.63 ± 0.08
7b	21.31 ± 0.19
7d	142.68 ± 0.08
7h	90.99 ± 0.19
8b	58.43 ± 0.07
8d	98.36 ± 0.02
8h	92.57 ± 0.03
Ascorbic acid	45.64 ± 0.05

* Data were expressed as the means of two determinations ± SEM.

Examination of the structure of the test compounds revealed that the starting pyrazole carboxaldehydes exhibited variable DPPH and NO scavenging potential. Compounds **4b** and **4d** comprising rhodanine with sulfonamide moiety demonstrated decrease in both DPPH and NO scavenging potencies. Whereas, compound **4a** revealed activities in both assays. In addition derivatives incorporating rhodanine with acetic acid fragment (**5a**, **5b** and **5d**) displayed higher DPPH scavenging activity than the precursor. Whereas, only compound **5a** showed higher NO scavenging potential. On the other hand, with the exception of **7d** cyclization of the thiosemicarbazones **6b**, **6d** and **6h** led to the thiazolines **7b** and **7h** and the thiazolidinones **8b**, **8d** and **8h** with much better DPPH scavenging potency and little or no improvement in NO scavenging activity.

2.3. Molecular docking studies

In the current study, several compounds showing potent 15-LOX inhibitory activity were chosen for molecular docking studies in the active binding site of the crystal structure of the 15-LOX enzyme (PDB ID code: 1LOX). Consequently, the mechanism of the inhibitory activity and possible interactions with the enzyme could be proposed in comparison with the co-crystallized ligand: RS7 [(*E*)-3-(2-(oct-1-yn-1-yl) phenyl)acrylic acid].

The proposed docking algorithm was validated by redocking of the co-crystallized ligand ***RS7*** into 15-LOX binding site. The initial poses generated from PDB were retrieved with root mean square deviation (RMSD) of 0.86 Å and docking score of −6.43 kcal/mol. This result indicated that Molecular Operating Environment (MOE) docking can predict the docking poses of the test compounds. It was reported that values less than 1.5 or 2 Å denotes successful and reliable docking protocol [39].

The co-crystallized ligand ***RS7*** bound to the active site of 15-LOX enzyme showed hydrogen bonding between OH of the carboxylic function (donor) and Leu 597 (acceptor). Also, hydrogen bonding was observed between with hydrogens of the phenyl ring and side chain and amino acid residues Met 419, Glu 357 and His 366 (Fig. 4). Docking score of the redocked RS7 in the 15-LOX active site was −6.43 kcal/mol. Docking of compound **4a** in the active site of the 15-LOX enzyme showed the formation of 5 hydrogen bond interactions between the ethyl side chain and the amino acid Ala 662 and between the sulfur atom of the rhodanine ring and two amino acids Leu 597 and Ile 663. Also, the sulfur and one of the oxygens of sulfonamide group acted as hydrogen bond acceptors with the amino acids Val 594 and Ile 593, respectively. In addition, three arene-hydrogen bonds stabilized the complex; between the pyrazole, imidazole and rhodanine rings and Ile 400 and two leu 597 respectively (Fig. 5). It had binding energy score of −2.27 kcal/mol. Observation of the binding interactions of compound **7b** (energy score of −7.58 kcal/mol) showed hydrogen bond formation as a H-donor between one methyl group and Met 419, the sulfur atom of the thiazolidine ring and Arg 403, the phenyl ring and Ile 663 and the oxygen atom at position 2 of the pyrimidine ring acted as an acceptor with Val 594. Additionally, a hydrogen-arene interaction is formed between imidazole ring and Leu 408 (Fig. 6). Moreover, the best binding conformation of compound **7d** (energy score of −6.35 kcal/mol) revealed hydrogen bonding between the amino acid residue Met 419 and the methyl group, also, Val 594 was hydrogen bonded with both the ethyl side chain and the oxygen atom at position 6 of the pyrimidine ring. Furthermore, two arene-hydrogen bonds were formed between the pyrazole ring and Leu 597 and the pyrimidine ring with Ile 593 (Fig. 7). Compound **7h** was successfully docked with score of −4.83 kcal/mol into the active site of 15-LOX with the formation of a hydrogen bond between the Val 594 with both the ethyl side chain and the oxygen atom at position 6 of the pyrimidine ring, as well the oxygen atom was bonded to Ile 593. Besides, Met 419 formed a hydrogen bond with the methyl group and Ala 404 acted as a hydrogen donor to the nitrogen atom of the hydrazone moiety. Over and above that, arene-hydrogen interactions were located between the pyrazole ring and Leu 597, the p-bromophenyl ring and Leu 362 and the phenyl ring and Leu 408 (Fig. 8). Furthermore, compound **8b** demonstrated hydrogen bonding interaction between Met 419 and the phenyl ring. Arg 599 acted as a hydrogen donor and acceptor with the oxygen atom on position 2 of the pyrimidine ring and the pyrimidine nitrogen atom, respectively. Similarly, Phe 175 and Phe 415 formed hydrogen bonds with oxygen atom at position 6 of the pyrimidine ring and with oxygen atom of the thiazolidinone moiety, respectively (Fig. 9). The docking score was −3.37 kcal/mol. Finally, compound **8d** exhibited hydrogen bonds between the chlorine atom and Ile 400, the thiazolidinone ring and Glu 357. Whereas, the oxygen atom showed three hydrogen bonds with Gln 548, Val 594 and Leu 597 (Fig. 10). The molecular modeling docking scores, amino acid residue interactions and the hydrogen bond lengths of the tested compounds were summarized in Table 5.

3. Experimental

3.1. Chemistry

All reagents and solvents were purchased from commercial suppliers and were dried and purified when necessary by standard techniques. Melting points were determined in open-glass capillaries using a Stuart SMP10-Barloworld melting point apparatus and are uncorrected. Follow up of the reactions progress were performed by thin-layer chromatography (TLC) on silica gel (60 GF254) coated glass plates and the spots were visualized by exposure to iodine vapors or UV-lamp at λ 254 nm for few seconds. Infrared spectra (IR) were recorded, for potassium bromide discs, on a PerkinElmer RXIFT-IR spectrometer and on Bruker Tensor 37 FT-IR spectrometer. Nuclear magnetic resonance spectra (^{1}H NMR) were scanned on Jeol 500 MHz spectrophotometer, on a Bruker Avance III FT-NMR 400 MHz spectrophotometer and on Varian Mercury VX 300 MHz spectrophotometer. The data were reported as δ values (ppm) relative to tetramethylsilane (TMS) as internal standard. The type of signals was indicated by one of the following letters: s = singlet, d = doublet, t = triplet, q = quartet, m = multiplet, dd = doublet of doublet, br. = broad and dist. = distorted. The results of microanalyses were within ± 0.4% of the calculated values for the proposed formulae.

3.1.1. *4-{5-{[3-Aryl-1-(7-ethyl-1,3-dimethyl-2,6-dioxo-2,3,6,7-tetrahydro-1H-purin-8-yl)-1H-pyrazol-4-yl]methylene}-4-oxo-2-thioxothiazolidin-3-yl} benzenesulfonamides* ***(4a-d)***

To a suspension of the appropriate 3a-d (1 mmol) and 4-(4-oxo-2-thioxothiazolidin-3-yl)benzenesulfonamide (0.29 g, 1 mmol) in dry dioxane (5 ml), two drops of piperidine were added and the reaction mixture was heated under reflux for 6 h. The precipitate formed was filtered, washed with dioxane, air dried and crystallized from dioxane.

3.1.1.1. 4-{5-{[1-(7-Ethyl-1,3-dimethyl-2,6-dioxo-2,3,6,7-tetrahydro-1H-purin-8-yl)-3-phenyl-1H-pyrazol-4-yl]methylene}-4-oxo-2-thioxothiazolidin-3-yl}benzenesulfonamide ***(4a)***. Yield 38%, m.p 296–298 °C. IR (KBr, cm^{-1}): 3430 (br. NH_2); 1702 (br. C=O rhodanine and purine); 1655 (C=O purine); 1621 (C=N); 1538, 1346 (SO_2); 1038 (C–S–C). ^{1}H NMR (300 MHz, DMSO-d_6, δ ppm): 1.45 (t, J = 6.9 Hz, 3H, $CH_2C\underline{H}_3$); 3.28 (s, 3H, purine-N_3-CH_3); 3.50 (s, 3H, purine-N_1-CH_3); 4.61 (q, J = 6.9 Hz, 2H, $C\underline{H}_2CH_3$); 7.49–7.70 (m, 10H, phenyl-$C_{2\text{-}6}$-H, benzenesulfonamide-$C_{2,6}$-H, C=CH and NH_2); 8.01 (d, J = 8.7 Hz, 2H, benzenesulfonamide-$C_{3,5}$-H); 8.75 (s, 1H, pyrazole-C_5 -H). Elemental analysis Calcd for $C_{28}H_{24}N_8O_5S_3$ (648.74): C, 51.84; H, 3.73; N, 17.27; S, 14.83. Found: C, 52.08; H, 3.71; N, 17.49; S, 14.91.

3.1.1.2. 4-{5-{[3-(4-Chlorophenyl)-1-(7-ethyl-1,3-dimethyl-2,6-dioxo-2,3,6,7-tetrahydro-1H-purin-8-yl)-1H-pyrazol-4-yl]methylene}-4-oxo-2-thioxothiazolidin-3-yl} benzenesulfonamide ***(4b)***. Yield 72%, m.p > 300 °C. IR (KBr, cm^{-1}): 3314, 3218 (NH_2); 1705 (br. C=O

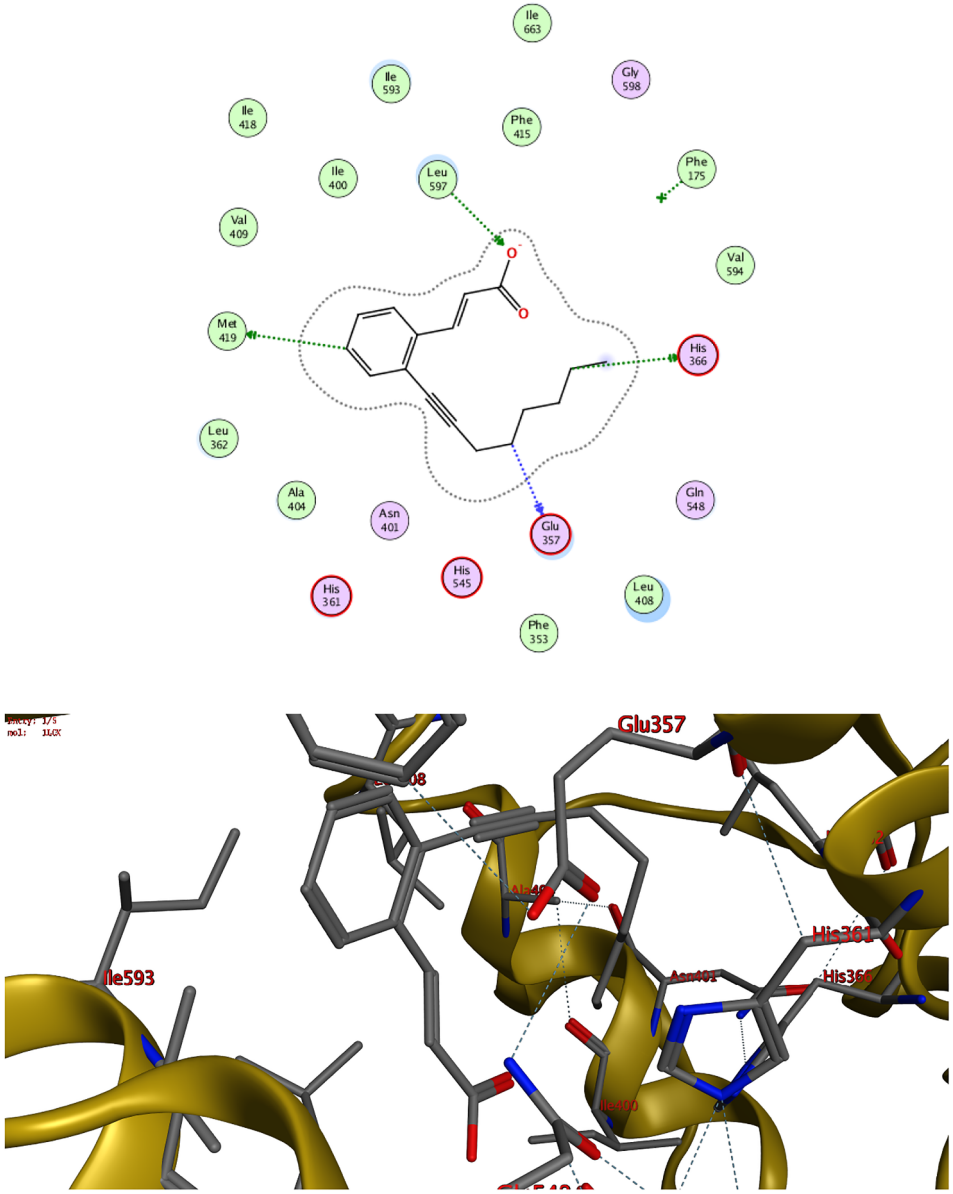

Fig. 4. Docking and binding pattern of RS7 into 15-LOX active site (PDB 1LOX) in 2D (upper panel) and 3D (lower panel).

rhodanine and purine); 1655 (C═O purine); 1608 (C═N); 1537, 1350 (SO_2); 1039 (C–S–C); 754 (C-Cl). ^{1}H NMR (300 MHz, DMSO-d_6, δ ppm): 1.53 (dist. t, 3H, $CH_2\underline{CH_3}$); 3.35 (s, 3H, purine-N_3-CH_3); 3.56 (s, 3H, purine-N_1-CH_3); 4.58 (dist. q, 2H, $\underline{CH_2}CH_3$); 7.64–7.72 (m, 9H, 4-chlorophenyl-$C_{2,3,5,6}$-H, benzenesulfonamide-$C_{2,6}$-H, C═CH and NH_2); 8.08–8.10 (m, 2H, benzenesulfonamide-$C_{3,5}$-H); 8.67 (s, 1H, pyrazole-C_5 -H). Elemental analysis Calcd for $C_{28}H_{23}ClN_8O_5S_3$ (683.18): C, 49.23; H, 3.39; N, 16.40; S, 14.08. Found: C, 49.51; H, 3.36; N, 16.73; S, 14.21.

3.1.1.3. 4-{5-{[1-(7-Ethyl-1,3-dimethyl-2,6-dioxo-2,3,6,7-tetrahydro-1H-purin-8-yl)-3-(4-methylphenyl)-1H-pyrazol-4-yl]methylene}-4-oxo-2-thioxothiazolidin-3-yl} benzenesulfonamide ***(4c)***. Yield 79%, m.p > 300 °C. IR (KBr, cm^{-1}): 3386 (br. NH_2); 1704 (br. C═O rhodanine and purine); 1659 (C═O purine); 1610 (C═N); 1540, 1347 (SO_2); 1096 (C–S–C). ^{1}H NMR (300 MHz, DMSO-d_6, δ ppm): 1.46 (t, J = 7.2 Hz, 3H, $CH_2\underline{CH_3}$); 2.39 (s, 3H, 4-methylphenyl-CH_3); 3.30 (s, 3H, purine-N_3-CH_3); 3.51 (s, 3H, purine-N_1-CH_3); 4.60 (q, J = 7.2 Hz, 2H, $\underline{CH_2}CH_3$); 7.39 (d, J = 7.7 Hz, 2H, 4-methylphenyl-$C_{3,5}$-H); 7.53 (s, 2H, NH_2, D_2O exchangeable); 7.57 (d, J = 7.7 Hz, 2H, 4-methylphenyl-$C_{2,6}$-H); 7.61 (s, 1H, C═CH); 7.66 (d, J = 8.4 Hz, 2H, benzenesulfonamide-$C_{2,6}$-H); 8.01 (d, J = 8.4 Hz, 2H, benzenesulfonamide- $C_{3,5}$-H); 8.72 (s, 1H, pyrazole-C_5 -H). Elemental analysis Calcd for $C_{29}H_{26}N_8O_5S_3$ (662.76): C, 52.55; H, 3.95; N, 16.91; S, 14.51. Found: C, 52.69; H, 3.98; N, 17.08; S, 14.62.

3.1.1.4. 4-{5-{[1-(7-Ethyl-1,3-dimethyl-2,6-dioxo-2,3,6,7-tetrahydro-1H-purin-8-yl)-3-(4-methoxyphenyl)-1H-pyrazol-4-yl]methylene}-4-oxo-2-thioxothiazolidin-3-yl} benzenesulfonamide ***(4d)***. Yield 48%, m.p > 300 °C. IR (KBr, cm^{-1}): 3239 (br. NH_2); 1703 (br. C═O rhodanine and purine); 1653 (C═O purine); 1608 (C═N); 1540, 1351 (SO_2); 1250 (C–O–C), 1041 (C–S–C). ^{1}H NMR (300 MHz, DMSO-d_6, δ ppm): 1.46 (t, J = 7.0 Hz, 3H, $CH_2\underline{CH_3}$); 3.27 (s, 3H, purine-N_3-CH_3); 3.46 (s, 3H, purine-N_1-CH_3); 3.81 (s, 3H, OCH_3); 4.58 (q, J = 7.0 Hz, 2H, $\underline{CH_2}CH_3$); 7.09 (d, J = 8.7 Hz, 2H, 4-methoxyphenyl-$C_{3,5}$-H); 7.53 (s, 2H, NH_2, D_2O exchangeable); 7.58 (d, J = 8.4 Hz, 2H, benzenesulfonamide-$C_{2,6}$-H); 7.63 (s, 1H, C═CH); 7.65 (d, J = 8.7 Hz, 2H, 4-methoxyphenyl-$C_{2,6}$-H,); 8.01 (d, J = 8.4 Hz, 2H, benzenesulfonamide-$C_{3,5}$-H); 8.63 (s, 1H, pyrazole-C_5 -H). ^{13}C NMR (75 MHz, $CDCl_3$/TFA, δ ppm): 15.84 ($CH_2\underline{CH_3}$); 29.06 (purine-N_3-CH_3);

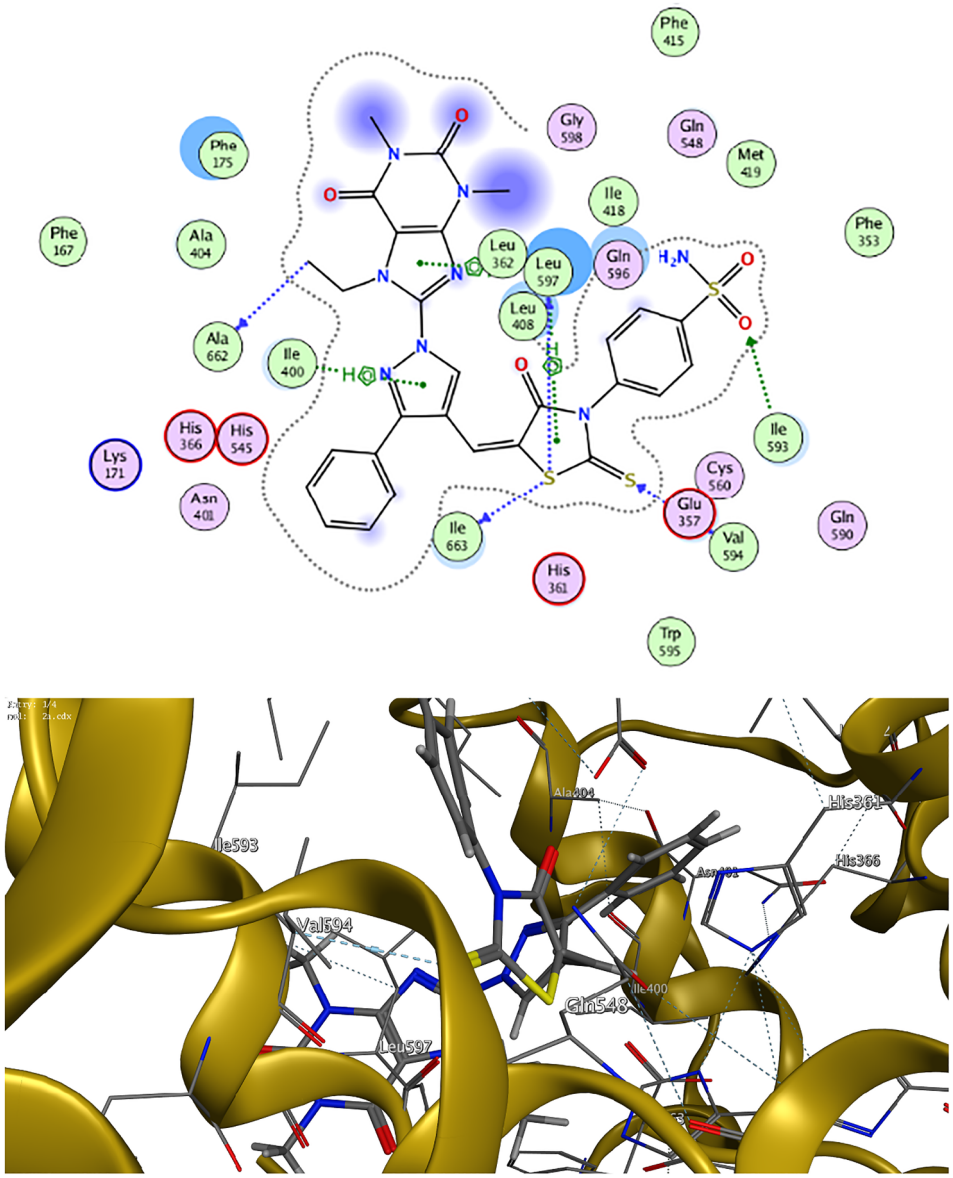

Fig. 5. Docking and binding pattern of compound **4a** into 15-LOX active site (PDB code: 1LOX) in 2D (upper panel) and 3D (lower panel).

30.76 (purine-N_1-CH_3); 43.52 ($\underline{C}H_2CH_3$); 55.65 (OCH_3); 108.75 (pyrazole-C_4); 114.78 (purine-C_5); 114.97 (4-methoxyphenyl-$C_{3,5}$); 117.09 (benzenesulfonamide-$C_{2,6}$); 122.55 (rhodanine-C_5); 123.93 (4-methoxyphenyl-C_1); 124.22 (4-methoxyphenyl-$C_{2,6}$); 127.90 (benzenesulfonamide-$C_{3,5}$); 129.79 (benzenesulfonamide-C_1); 130.30 (benzenesulfonamide-C_4); 132.02 (pyrazole-C_5); 138.61 (C═CH); 142.36 (pyrazole-C_3); 142.95 (purine-C_8); 147.31 (purine-C_4); 152.40 (4-methoxyphenyl-C_4); 155.28 (purine-C_2); 156.98 (purine-C_6); 167.74 (rhodanine-C_4═O); 190.56 (rhodanine-C_2 = S). Elemental analysis Calcd for $C_{29}H_{26}N_8O_6S_3$ (678.76):C, 51.32; H, 3.86; N, 16.51; S, 14.17. Found: C, 51.47; H, 3.85; N, 16.64; S, 14.25.

*3.1.2. 2-{5-{[3-Aryl-1-(7-ethyl-1,3-dimethyl-2,6-dioxo-2,3,6,7-tetrahydro-1H-purin-8-yl)-1H-pyrazol-4-yl]methylene}-4-oxo-2-thioxothiazolidin-3-yl}acetic acids (**5a-d**)*

To a mixture of the appropriate **3a-d** (1 mmol) and 2-(4-oxo-2-thioxothiazolidin-3-yl)acetic acid (0.19 g, 1 mmol) in dry dioxane (5 ml), ammonium acetate (0.08 g, 1.1 mmol) was added and the reaction mixture was heated under reflux for 4 h, then diluted with water. The precipitate formed was filtered, washed with water, air dried and crystallized from DMF/water.

*3.1.2.1. 2-{5-{[1-(7-Ethyl-1,3-dimethyl-2,6-dioxo-2,3,6,7-tetrahydro-1H-purin-8-yl)-3-phenyl-1H-pyrazol-4-yl]methylene}-4-oxo-2-thioxothiazolidin-3-yl}acetic acid (**5a**)*. Yield 71%, m.p > 300 °C. IR (KBr, cm^{-1}): 3472 (OH); 1725 (C═O acid); 1693 (br. C═O rhodanine and purine); 1656 (C═O purine); 1585 (C═N); 1296, 1043 (C−S−C). ^{1}H NMR (300 MHz, DMSO-d_6, δ ppm): 1.43 (t, J = 6.9 Hz, 3H, $CH_2\underline{CH_3}$); 3.27 (s, 3H, purine-N_3-CH_3); 3.49 (s, 3H, purine-N_1-CH_3); 4.56–4.63 (m, 4H, $\underline{CH_2}CH_3$ and $\underline{CH_2}COOH$); 7.56–7.58 (m, 4H, phenyl-$C_{3,4,5}$-H and C═CH); 7.65–7.68 (m, 2H, phenyl-$C_{2,6}$ -H); 8.67 (s, 1H, pyrazole-C_5-H). Elemental analysis Calcd for $C_{24}H_{21}N_7O_5S_2$ (551.60): C, 52.26; H, 3.84; N, 17.78; S, 11.63. Found: C, 52.43; H, 3.88; N, 18.01; S, 11.68.

*3.1.2.2. 2-{5-{[3-(4-Chlorophenyl)-1-(7-ethyl-1,3-dimethyl-2,6-dioxo-2,3,6,7-tetrahydro-1H-purin-8-yl)-1H-pyrazol-4-yl]methylene}-4-oxo-2-thioxothiazolidin-3-yl}acetic acid (**5b**)*. Yield 77%, m.p > 300 °C. IR

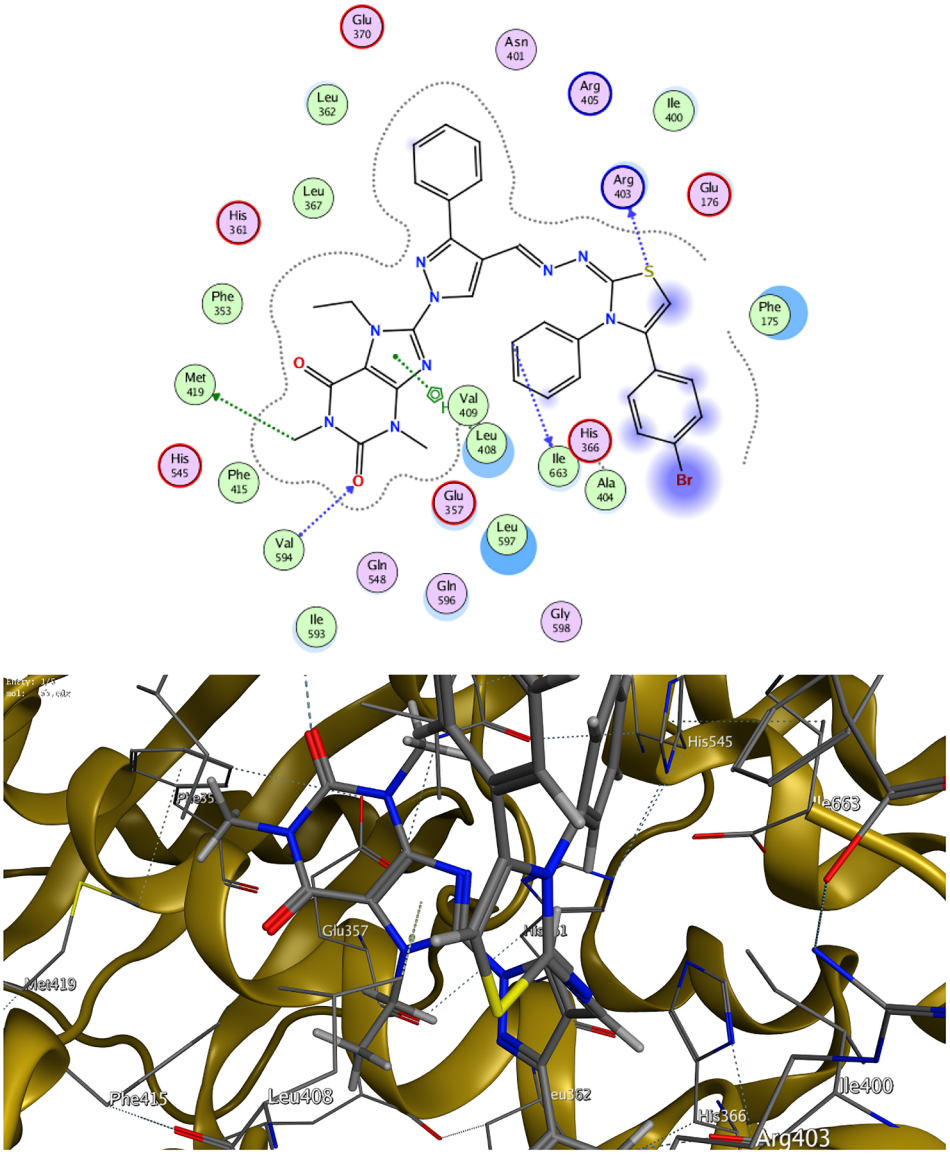

Fig. 6. Docking and binding pattern of compound **7b** into 15-LOX active site (PDB code: 1LOX) in 2D (upper panel) and 3D (lower panel).

(KBr, cm^{-1}): 3442 (OH); 1704 (br. C=O acid, C=O rhodanine and purine); 1662 (C=O purine); 1607 (C=N); 1038 (C–S–C); 752 (C-Cl). ^{1}H NMR (500 MHz, DMSO-d_6, δ ppm): 1.4 (t, J = 6.9 Hz, 3H, $CH_2\underline{CH_3}$); 3.23 (s, 3H, purine- N_3-CH_3); 3.44 (s, 3H, purine-N_1-CH_3); 4.51 (q, J = 6.9 Hz, 2H, $\underline{CH_2}CH_3$); 4.63 (s, 2H, $\underline{CH_2}COOH$); 7.53 (s, 1H, C=CH); 7.57 (d, J = 8.4 Hz, 2H, 4-chlorophenyl-$C_{2,6}$-H); 7.65 (d, J = 8.4 Hz, 2H, 4-chlorophenyl-$C_{3,5}$-H); 8.57 (s, 1H, pyrazole-C_5-H). Elemental analysis Calcd for $C_{24}H_{20}ClN_7O_5S_2$ (586.04): C, 49.19; H, 3.44; N, 16.73; S, 10.94. Found: C, 49.42; H, 3.46; N, 16.95; S, 11.02.

3.1.2.3. 2-{5-{[1-(7-Ethyl-1,3-dimethyl-2,6-dioxo-2,3,6,7-tetrahydro-1H-purin-8-yl)-3-(4-methylphenyl)-1H-pyrazol-4-yl]methylene}-4-oxo-2-thioxothiazolidin-3-yl}acetic acid ***(5c)***. Yield 97%, m.p 282–284 °C. IR (KBr, cm^{-1}): 3444 (br. OH); 1704 (br. C=O acid, C=O rhodanine and purine); 1661 (C=O purine); 1611 (C=N); 1042 (C–S–C). ^{1}H NMR (500 MHz, DMSO-d_6, δ ppm): 1.4 (t, J = 4.2 Hz, 3H, $CH_2\underline{CH_3}$); 2.33 (s, 3H, 4-methylphenyl-CH_3); 3.23 (s, 3H, purine-N_3-CH_3); 3.44 (s, 3H, purine-N_1-CH_3); 4.53 (q, J = 4.2 Hz, 2H, $\underline{CH_2}CH_3$); 4.68 (s, 2H, $\underline{CH_2}COOH$); 7.30 (d, J = 7.6 Hz, 2H, 4-methylphenyl-$C_{3,5}$-H); 7.48 (d, J = 7.6 Hz, 2H, 4-methylphenyl-$C_{2,6}$-H); 7.56 (s, 1H, C=CH); 8.57 (s, 1H, pyrazole-C_5-H); 13.0 (s, 1H, OH, D_2O exchangeable). Elemental analysis Calcd for $C_{25}H_{23}N_7O_5S_2$ (565.62): C, 53.09; H, 4.10; N, 17.33; S, 17.33. Found: C, 53.40; H, 4.17; N, 17.48; S, 11.41.

3.1.2.4. 2-{5-{[1-(7-Ethyl-1,3-dimethyl-2,6-dioxo-2,3,6,7-tetrahydro-1H-purin-8-yl)-3-(4-methoxyphenyl)-1H-pyrazol-4-yl]methylene}-4-oxo-2-thioxothiazolidin-3-yl}acetic acid ***(5d)***. Yield 43%, m.p 292–294 °C. IR (KBr, cm^{-1}): 3439 (OH); 1698 (br. C=O acid, C=O rhodanine and purine); 1659 (C=O purine); 1612 (C=N); 1218 (C–O–C); 1044 (C–S–C). ^{1}H NMR (300 MHz, DMSO-d_6, δ ppm): 1.43 (t, J = 7.0 Hz, 3H, $CH_2\underline{CH_3}$); 3.26 (s, 3H, purine-N_3-CH_3); 3.49 (s, 3H, purine-N_1-CH_3); 3.83 (s, 3H, OCH_3); 4.48 (s, 2H, $\underline{CH_2}COOH$); 4.57 (q, J = 7.0 Hz, 2H, $\underline{CH_2}CH_3$); 7.08 (d, J = 8.6 Hz, 2H, 4-methoxyphenyl-$C_{3,5}$-H); 7.52 (s, 1H, C=CH); 7.55 (d, J = 8.6 Hz, 2H, 4-methoxyphenyl-$C_{2,6}$-H); 8.52 (s, 1H, pyrazole-C_5-H). Elemental analysis Calcd for $C_{25}H_{23}N_7O_6S_2$ (581.62): C, 51.63; H, 3.99; N, 16.86; S, 11.03. Found: C, 51.79; H, 3.97; N, 16.98; S, 11.12.

3.1.3. 8-{4-{{[3-Aryl-4-(4-bromophenyl)-3-substituted thiazol-2(3H)-ylidene] hydrazono}-methyl}-1H-pyrazol-1-yl}-7-ethyl-1,3-dimethyl-1H-purine-2,6(3H,7H)-diones ***(7a-h)***

To a suspension of the appropriate thiosemicarbazone **6a-d** added. The reaction mixture was heated under reflux for 4 h, concentrated to

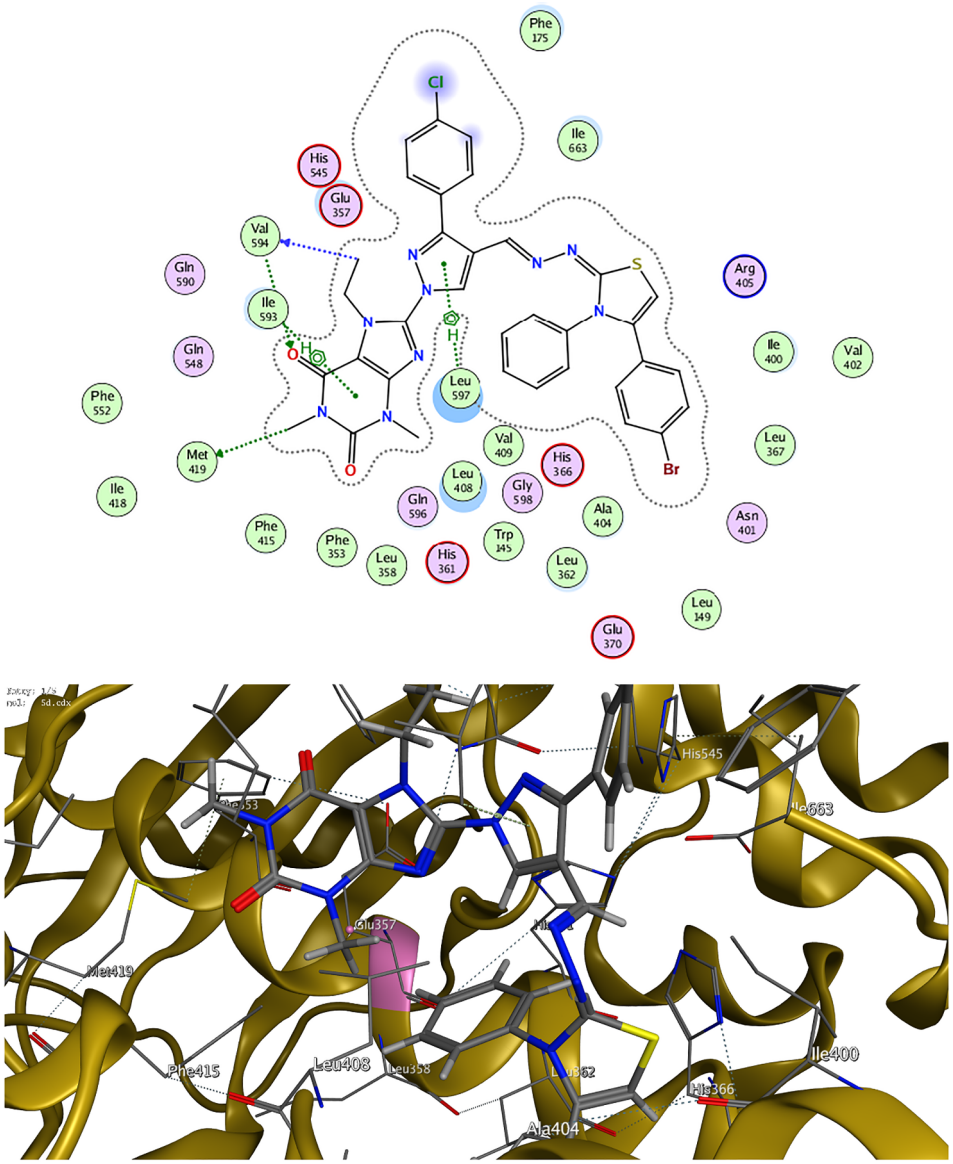

Fig. 7. Docking and binding pattern of compound **7d** into 15-LOX active site (PDB code: 1LOX) in 2D (upper panel) and 3D (lower panel).

small volume and cooled to room temperature. The product separated was filtered, washed with water followed by cold ethanol, air dried and crystallized from dioxane/ethanol.

*3.1.3.1. 8-{4-{{[4-(4-Bromophenyl)thiazol-2(3H)-ylidene]hydrazono} methyl}-3-phenyl-1H-pyrazol-1-yl}-7-ethyl-1,3-dimethyl-1H-purine-2,6(3H,7H)-dione (**7a**).* Yield 64%, m.p 176–178 °C. IR (KBr, cm^{-1}): 3221 (NH); 1702,1658 (C=O purine); 1562 (C=N); 1293, 1037 (C–S–C); 708 (C-Br). ^{1}H NMR (500 MHz, DMSO-d_6, δ ppm): 1.42 (t, J = 6.9 Hz, 3H, $CH_2C\underline{H}_3$); 3.19 (s, 3H, purine-N_3-CH_3); 3.41 (3H of purine-N_1-CH_3 congregated with the solvent absorption); 4.61 (q, J = 6.9 Hz, 2H, $C\underline{H}_2CH_3$); 7.32 (s, 1H, thiazoline-C_5-H); 7.43–7.58 (m, 5H, 4-bromophenyl-$C_{2,6}$-H and phenyl-$C_{3,4,5}$-H); 7.67–7.78 (m, 4H, 4-bromophenyl-$C_{3,5}$-H and phenyl-$C_{2,6}$-H); 8.08 (s, 1H, pyrazole-C_5 -H); 8.60 (s, 1H, N=CH); 12.01 (s, 1H, NH, D_2O exchangeable). Elemental analysis Calcd for $C_{28}H_{24}BrN_9O_2S$ (630.52): C, 53.34; H, 3.84; N, 19.99; S, 5.09. Found: C, 53.49; H, 3.87; N, 20.17; S, 5.16.

*3.1.3.2. 8-{4-{{[4-(4-Bromophenyl)-3-phenylthiazol-2(3H)-ylidene] hydrazono}methyl}-3-phenyl-1H-pyrazol-1-yl}-7-ethyl-1,3-dimethyl-1H-purine-2,6(3H,7H)-dione (**7b**).* Yield 67%, m.p 294–296 °C. IR (KBr, cm^{-1}): 1703, 1658 (C=O purine); 1607 (C=N); 1295, 1035 (C–S–C); 700 (C-Br). ^{1}H NMR (300 MHz, DMSO-d_6, δ ppm): 1.40 (t, J = 7.1 Hz, 3H, $CH_2C\underline{H}_3$); 3.28 (3H of purine-N_3-CH_3 congregated with the solvent absorption); 3.56 (s, 3H, purine-N_1-CH_3); 4.54 (q, J = 7.1 Hz, 2H, $C\underline{H}_2CH_3$); 6.81 (s, 1H, thiazoline-C_5-H); 7.16 (d, J = 8.7 Hz, 2H, 4-bromophenyl-$C_{2,6}$-H); 7.26–7.37 (m, 1H, *N*-phenyl-C_4-H); 7.39–7.57 (m, 10*H*, pyrazole-C_5-H, 4-bromophenyl-$C_{3,5}$-H, phenyl-$C_{3,4,5}$-H and *N*-phenyl-$C_{2,3,5,6}$-H); 7.68 (dd, J = 9.0, 1.7 Hz, 2H, phenyl-$C_{2,6}$-H); 8.63 (s, 1H, N=CH). Elemental analysis Calcd for $C_{34}H_{28}BrN_9O_2S$ (706.61): C, 57.79; H, 3.99; N, 17.84; S, 4.54. Found: C, 57.98; H, 4.01; N, 18.09; S, 4.62.

*3.1.3.3. 8-{4-{{[4-(4-Bromophenyl)thiazol-2(3H)-ylidene]hydrazono} methyl}-3-(4-chlorophenyl)-1H-pyrazol-1-yl}-7-ethyl-1,3-dimethyl-1H-purine-2,6(3H,7H)-dione (**7c**).* Yield 65%, m.p 179–181 °C. IR (KBr, cm^{-1}): 3206 (NH); 1703, 1649 (C=O purine); 1562 (C=N); 1290, 1039 (C–S–C); 729 (C-Cl); 685 (C-Br). ^{1}H NMR (300 MHz, DMSO-d_6, δ ppm): 1.45 (t, J = 6.7 Hz, 3H, $CH_2C\underline{H}_3$); 3.23 (s, 3H, purine-N_3-CH_3); 3.45 (s, 3H, purine-N_1-CH_3); 4.64 (q, J = 6.7 Hz, 2H, $C\underline{H}_2CH_3$); 7.34 (s, 1H, thiazoline-C_5-H) 7.53–7.61 (m, 4H, 4-bromophenyl-$C_{2,3,5,6}$-H); 7.75 (d, J = 8.3 Hz, 2H, 4-chlorophenyl-$C_{2,6}$-H); 7.82 (d, J = 8.3 Hz, 2H, 4-

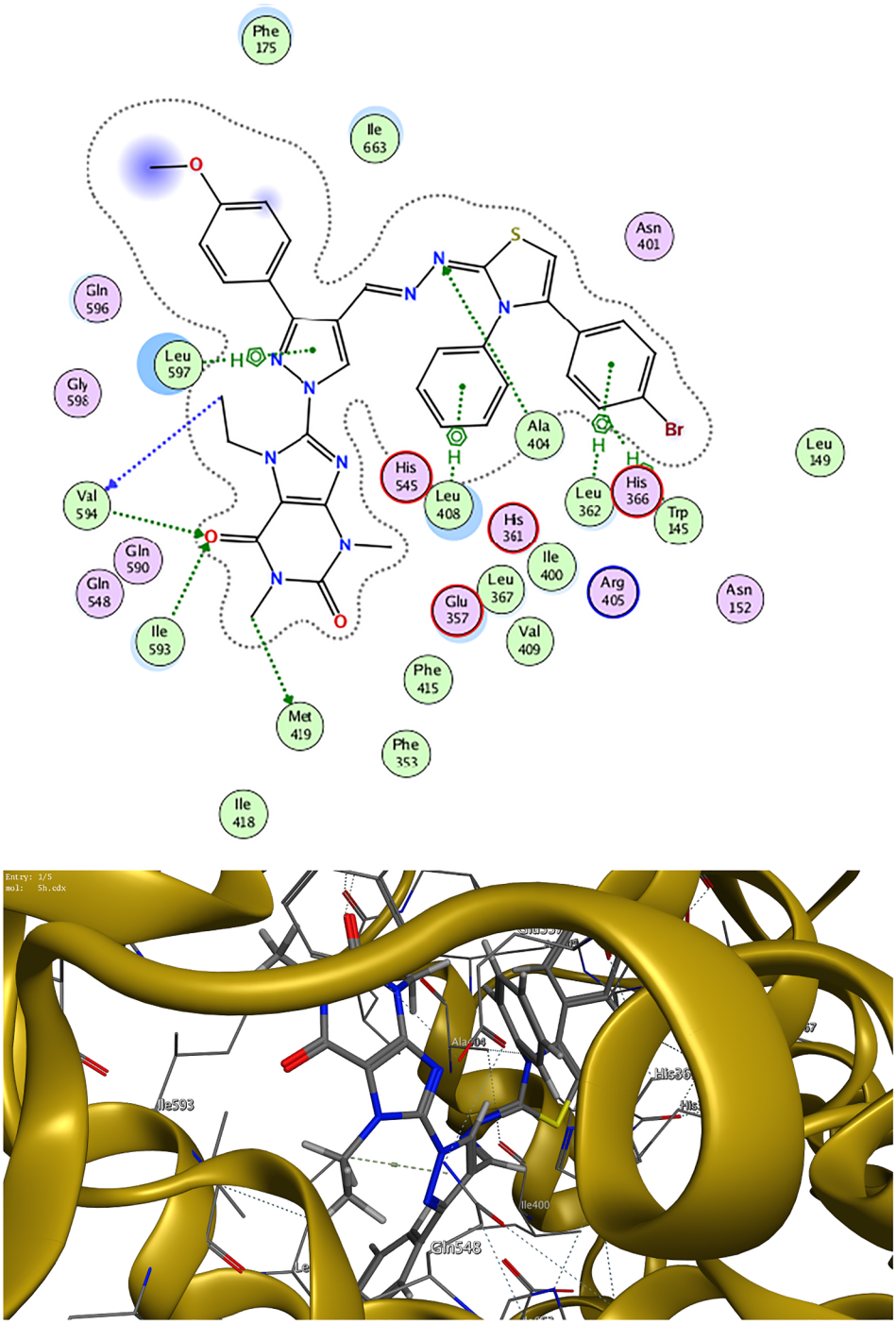

Fig. 8. Docking and binding pattern of compound **7h** into 15-LOX active site (PDB code: 1LOX) in 2D (upper panel) and 3D (lower panel).

chlorophenyl-$C_{3,5}$-H); 8.11 (s, 1H, pyrazole- C_5-H); 8.66 (s, 1H, N=CH); 12.02 (s, 1H, NH, D_2O exchangeable). Elemental analysis Calcd for $C_{28}H_{23}BrClN_9O_2S$

(664.96): C, 50.57; H, 3.49; N, 18.96; S, 4.82. Found: C, 50.74; H, 3.52; N, 19.12; S, 4.91.

*3.1.3.4. 8-{4-{{[4-(4-Bromophenyl)-3-phenylthiazol-2(3H)-ylidene] hydrazono}methyl}-3-(4-chlorophenyl)-1H-pyrazol-1-yl}-7-ethyl-1,3-dimethyl-1H-purine-2,6(3H,7H)-dione (**7d**).* Yield 64%, m.p 285–287 °C. IR (KBr, cm^{-1}): 1700, 1657 (C=O purine); 1612 (C=N); 1292, 1084 (C−S−C); 747 (C-Cl); 697 (C-Br). ^1H NMR (400 MHz, DMSO-d_6, δ ppm): 1.46 (t, J = 6.9 Hz, 3H, $CH_2\underline{CH}_3$); 3.28 (s, 3H, purine-N_3-CH_3); 3.47 (s, 3H, purine-N_1-CH_3); 4.66 (q, J = 6.9 Hz, 2H, $\underline{CH}_2CH_3$); 6.72 (s, 1H, thiazoline-C_5-H); 7.11 (d, J = 8.4 Hz, 2H, 4-bromophenyl-$C_{2,6}$-H); 7.28 (d, J = 7.3 Hz, 2H, *N*-phenyl-$C_{2,6}$-H); 7.33 (dist. t, J = 7.3 Hz, 1H, *N*-phenyl-C_4-H); 7.40 (t, J = 7.3 Hz, 2H, *N*-phenyl-$C_{3,5}$-H); 7.45 (d, J = 8.4 Hz, 2H, 4-bromophenyl-$C_{3,5}$-H); 7.60 (d, J = 8.4 Hz, 2H, 4-chlorophenyl-$C_{2,6}$-H); 7.97 (d, J = 8.4 Hz, 2H, 4-chlorophenyl-$C_{3,5}$-H); 8.25 (s, 1H, pyrazole- C_5-H); 8.73 (s, 1H, N=CH). Elemental analysis Calcd for $C_{34}H_{27}BrClN_9O_2S$ (741.06): C, 55.11; H, 3.67; N, 17.01; S, 4.33. Found: C, 55.34; H, 3.72; N, 17.18; S, 4.40.

*3.1.3.5. 8-{4-{{[4-(4-Bromophenyl)thiazol-2(3H)-ylidene]hydrazono} methyl}-3-(4-methyl- phenyl)-1H-pyrazol-1-yl}-7-ethyl-1,3-dimethyl-1H-purine-2,6(3H,7H)-dione (**7e**).* Yield 80%, m.p 278–280 °C. IR (KBr, cm^{-1}): 3202 (NH); 1702, 1647 (C=O purine); 1569 (C=N); 1248,

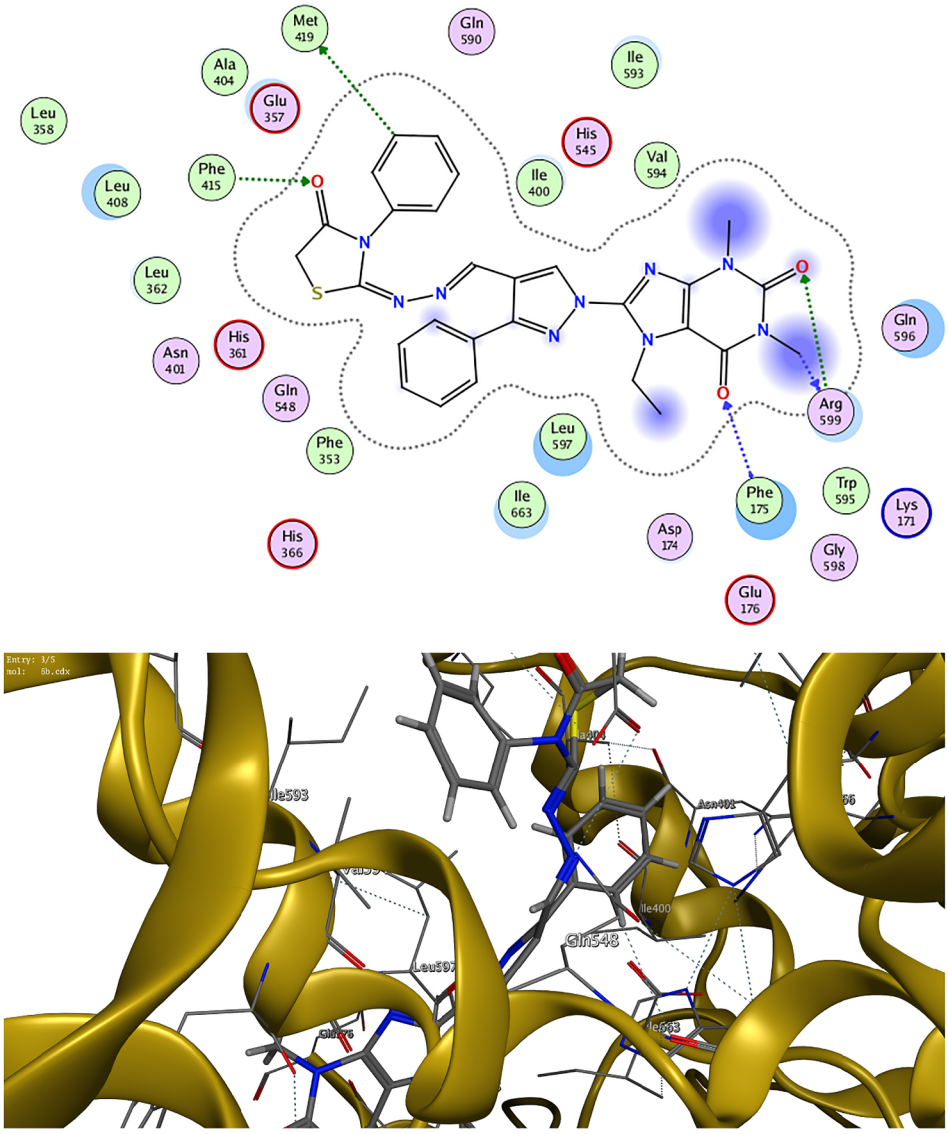

Fig. 9. Docking and binding pattern of compound **8b** into 15-LOX active site (PDB code: 1LOX) in 2D (upper panel) and 3D (lower panel).

1038 (C—S—C); 685 (C-Br). ^{1}H NMR (300 MHz, DMSO-d_6, δ ppm): 1.45 (t, J = 6.8 Hz, 3H, $CH_2\underline{CH_3}$); 2.39 (s, 3H, 4-methylphenyl-CH_3); 3.24 (s, 3H, purine-N_3-CH_3); 3.46 (s, 3H, purine-N_1-CH_3); 4.66 (q, J = 6.8 Hz, 2H, $C\underline{H_2}CH_3$); 7.32 (s, 1H, thiazoline-C_5-H); 7.35 (br. s, 2H, 4-bromophenyl-$C_{2,6}$-H); 7.57 (d, J = 7.3 Hz, 2H, 4-methylphenyl-$C_{3,5}$-H); 7.66 (d, J = 6.9 Hz, 2H, 4-bromophenyl-$C_{3,5}$-H); 7.77 (d, J = 7.3 Hz, 2H, 4-methylphenyl-$C_{2,6}$-H); 8.13 (s, 1H, pyrazole-C_5-H); 8.62 (s, 1H, N=CH); 12.01 (s, 1H, NH, D_2O exchangeable). Elemental analysis Calcd for $C_{29}H_{26}BrN_9O_2S$ (644.54): C, 54.04; H, 4.07; N, 19.56; S, 4.97. Found: C, 54.23; H, 4.11; N, 19.78; S, 5.01.

*3.1.3.6. 8-{4-{{[4-(4-Bromophenyl)-3-phenylthiazol-2(3H)-ylidene] hydrazono}methyl}-3-(4-methylphenyl)-1H-pyrazol-1-yl}-7-ethyl-1,3-dimethyl-1H-purine-2,6(3H,7H)-dione (**7f**).* Yield 83%, m.p 254–256 °C. IR (KBr, cm^{-1}): 1702, 1659 (C=O purine); 1614 (C=N); 1296, 1034 (C—S—C); 697 (C-Br). ^{1}H NMR (300 MHz, DMSO-d_6, δ ppm): 1.39, 1.45 (2 t, J = 6.9 Hz, 3H, $CH_2\underline{CH_3}$, E & Z isomers); 2.37, 2.38 (2 s, 3H, 4-methylphenyl-CH_3, E & Z isomers); 3.27, 3.29 (2 s, 3H, purine-N_3-CH_3, E & Z isomers); 3.47, 3.55 (2 s, 3H, purine-N_1-CH_3, E & Z isomers); 4.53, 4.67 (2q, J = 6.9 Hz, 2H, $C\underline{H_2}CH_3$, E & Z isomers); 6.71, 6.80 (2s, 1H, thiazoline-C_5-H, E & Z isomers); 7.10, 7.15 (2d, J = 7.1 Hz, 2H, phenyl-$C_{2,6}$-H, E & Z isomers); 7.26–7.48 (m, 9H, 4-bromophenyl-$C_{2,3,5,6}$-H, 4-methylphenyl-$C_{3,5}$-H and phenyl-$C_{3,4,5}$-H); 7.54, 7.75 (2d, J = 6.2 Hz, 2H, 4-methylphenyl-$C_{2,6}$-H, E & Z isomers); 7.55, 8.19 (2 s, 1H, pyrazole-C_5-H, E & Z isomers); 8.60, 8.67 (2 s, 1H, N=CH, E & Z isomers). Elemental analysis Calcd for $C_{35}H_{30}BrN_9O_2S$ (720.64): C, 58.33; H, 4.20; N, 17.49; S, 4.45. Found: C, 58.61; H, 4.28; N, 17.75; S, 4.59.

*3.1.3.7. 8-{4{{[4-(4-Bromophenyl)thiazol-2(3H)-ylidene]hydrazono} methyl}-3-(4-methoxy- phenyl)-1H-pyrazol-1-yl}-7-ethyl-1,3-dimethyl-1H-purine-2,6(3H,7H)-dione (**7g**).* Yield 60%, m.p 192–194 °C. IR (KBr, cm^{-1}): 3199 (NH); 1700, 1649 (C=O purine); 1578 (C=N); 1249 (C—O—C); 1037 (C—S—C); 688 (C-Br). ^{1}H NMR (300 MHz, DMSO-d_6, δ ppm): 1.45 (t, J = 6.7 Hz, 3H, $CH_2\underline{CH_3}$); 3.23 (s, 3H, purine-N_3-CH_3); 3.45 (s, 3H, purine-N_1-CH_3); 3.83 (s, 3H, OCH_3); 4.91 (q, J = 6.7 Hz, 2H, $C\underline{H_2}CH_3$); 7.06 (d, J = 8.7 Hz, 2H, 4-methoxyphenyl-$C_{3,5}$-H); 7.34 (s, 1H, thiazoline-C_5-H); 7.56 (d, J = 8.4 Hz, 2H, 4-bromophenyl-$C_{2,6}$-H); 7.69–7.77 (m, 4H, 4-bromophenyl-$C_{3,5}$-H and 4-methoxyphenyl-$C_{2,6}$-H); 8.12 (s, 1H, pyrazole-C_5-H); 8.59 (s, 1H, N=CH); 12.0 (s, 1H, NH, D_2O exchangeable). Elemental analysis Calcd for $C_{29}H_{26}BrN_9O_3S$ (660.54): C, 52.73; H, 3.97; N, 19.08; S, 4.85. Found: C, 52.87; H, 4.01; N, 19.31; S, 4.92.

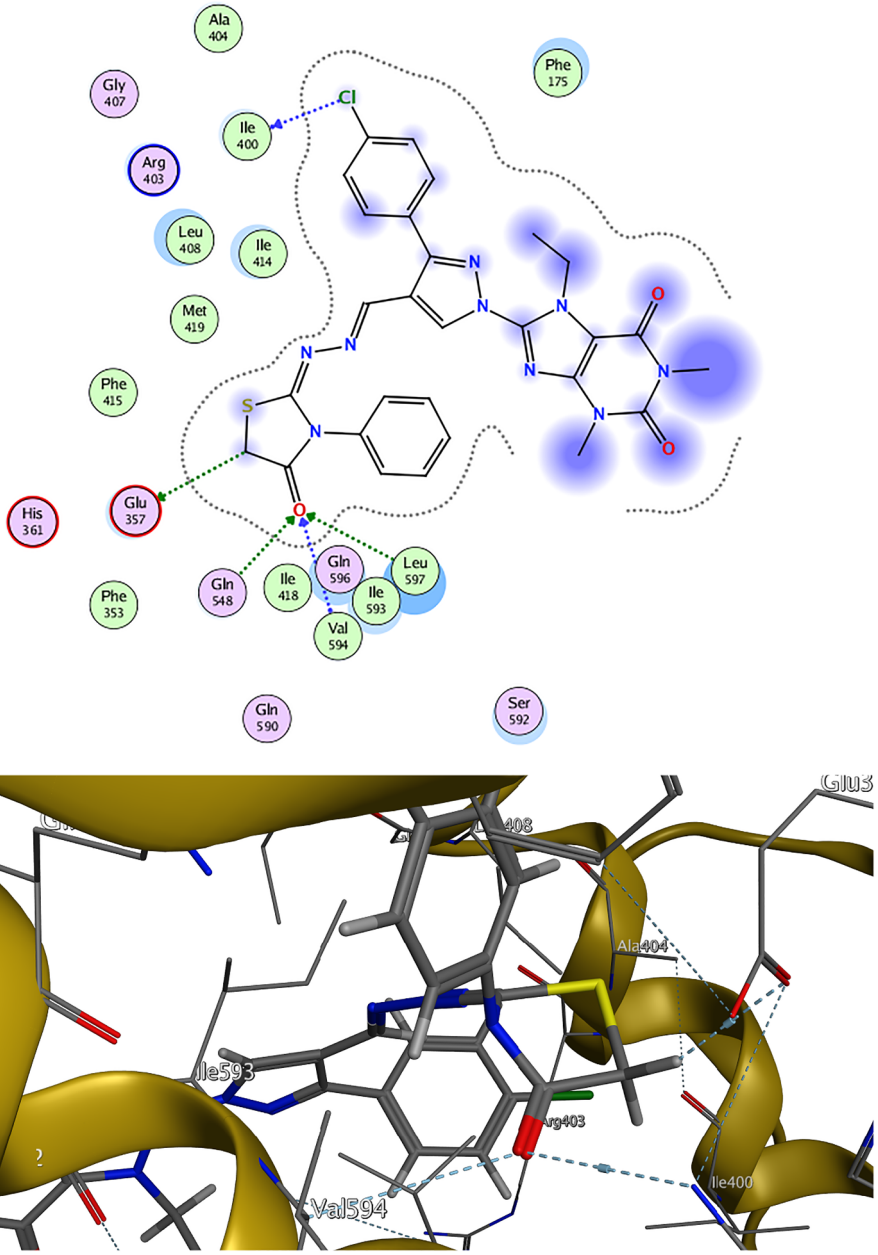

Fig. 10. Docking and binding pattern of compound **8d** into 15-LOX active site (PDB code: 1LOX) in 2D (upper panel) and 3D (lower panel).

*3.1.3.8. 8-{4-{{[4-(4-Bromophenyl)-3-phenylthiazol-2(3H)-ylidene] ydrazono}methyl}-3-(4-methoxyphenyl)-1H-pyrazol-1-yl}-7-ethyl-1,3-dimethyl-1H-purine-2,6(3H,7H)-dione (**7h**).* Yield 57%, m.p 229–231 °C. IR (KBr, cm^{-1}): 1698, 1657 (C═O purine); 1613 (C═N); 1246 (C–O–C); 1029 (C–S–C); 694 (C-Br). ^{1}H NMR (300 MHz, DMSO-d_6, δ ppm): 1.25, 1.58 (2 t, J = 6.4 Hz, 3H, $CH_2\underline{CH}_3$, E & Z isomers); 3.46, 3.48 (2 s, 3H, purine-N_3-CH_3, E & Z isomers); 3.63, 3.69 (2 s, 3H, purine-N_1-CH_3, E & Z isomers); 3.86, 3.88 (2 s, 3H, OCH_3, E & Z isomers); 4.72, 4.91 (2q, J = 6.4 Hz, 2H, $C\underline{H}_2CH_3$, E & Z isomers); 6.45, 6.67 (2 s, 1H, thiazoline-C_5-H, E & Z isomers); 6.97–7.07 (m, 4H, 4-methoxyphenyl- $C_{3,5}$-H and 4-bromophenyl-$C_{2,6}$-H); 7.28–7.35 (m, 2H, phenyl-$C_{2,6}$-H); 7.36–7.42 (m, 2H, 4-methoxyphenyl-$C_{2,6}$-H); 7.52–7.58 (m, 3H, phenyl-$C_{3,4,5}$-H); 7.76,7.84 (2d, J = 8.3 Hz, 2H, 4-bromophenyl-$C_{3,5}$-H, E & Z isomers); 8.67, 8.86 (2 s, 1H, pyrazole-C_5-H, E & Z isomers); 9.48, 10.12 (2 s, 1H, N═CH, E & Z isomers). Elemental analysis Calcd for $C_{35}H_{30}BrN_9O_3S$ (736.64): C, 57.07; H, 4.10; N, 17.11; S, 4.35. Found: C, 57.39; H, 4.17; N, 17.42; S, 4.33.

*3.1.4. 8-{3-Aryl-4-{[(3-substituted 4-oxothiazolidin-2-ylidene)hydrazono] methyl}-1H-pyrazol-1-yl}-7-ethyl-1,3-dimethyl-1H-purine-2,6(3H,7H)-diones (**8a-h**)*

A mixture of the appropriate thiosemicarbazone **6a-h** (1 mmol) and ethyl bromoacetate (0.17 g, 0.11 ml, 1 mmol) in dry dioxane (10 ml) containing anhydrous sodium acetate (0.08 g, 1 mmol) was heated under reflux for 4 h. The reaction mixture was then concentrated to small volume, and cooled to room temperature. The precipitate formed was filtered, washed with water followed by cold ethanol, air dried and crystallized from dioxane/ethanol.

*3.1.4.1. 7-Ethyl-1,3-dimethyl-8-{4-{[(4-oxothiazolidin-2-ylidene) hydrazono]methyl}-3-phenyl-1H-pyrazol-1-yl}-1H-purine-2,6(3H,7H)-dione (**8a**).* Yield 77%, m.p > 300 °C. IR (KBr, cm^{-1}): 3263 (NH); 1701 (br. C═O thiazolidinone and purine); 1661 (C═O purine); 1635 (C═N); 1292, 1031 (C–S–C). ^{1}H NMR (400 MHz, DMSO-d_6, δ ppm): 1.45 (t, J = 6.9 Hz, 3H, $CH_2\underline{CH}_3$); 3.26 (s, 3H, purine-N_3-CH_3); 3.46 (s, 3H, purine-N_1-CH_3); 3.89 (s, 2H, thiazolidinone-C_5-H); 4.66 (q,

Table 5
Molecular modeling results for the tested compounds and redocked ligand during docking in the 15-LOX enzyme (PDB: 1LOX).

Compound ID	E-score	No. of hydrogen bonds	Hydrogen bonding residues	Distance Å	H-bond E-score Kcal/mol
4a	−2.27	5	Ala 662	3.49	−0.3
			Leu 597	2.79	5.7
			Ile 663	4.50	−0.0
			Val 594	3.32	−1.0
			Ile 593	3.20	0.6
7b	−7.58	5	Met 419	4.06	−0.3
			Arg 403	3.11	1.2
			Ile 663	3.22	0.8
			Val 594	3.62	−0.5
				3.31	−0.1
7d	−6.35	3	Met 419	3.19	−0.5
			Val 594	3.36	−0.5
				3.06	1.8
7h	−4.83	5	Met 419	3.24	−0.6
			Val 594	3.29	−0.5
			Ile 593	3.12	1.2
			Val 594	2.82	8.1
			Ala 404	3.21	−0.3
8b	−3.37	5	Arg 599	3.50	−0.2
			Met 419	4.58	−0.2
			Phe 175	3.11	−1.1
			Arg 599	3.74	−0.3
			Phe 415	3.18	0.0
8d	−4.15	5	Glu 357	3.50	−0.7
			Ile 400	3.12	−0.1
			Gln 548	3.06	−1.2
			Val 594	3.81	−0.5
			Leu 597	3.39	−0.3
Ligand	−6.43	4	Met 419	4.17	−0.3
			Glu 357	3.31	−0.1
			His 366	3.59	−0.3
			Leu 597	3.33	−0.3

J = 6.9 Hz, 2H, C$\underline{H}_2$CH$_3$); 7.46–7.55 (m, 3H, phenyl-C$_{3,4,5}$-H); 7.88 (d, J = 6.6 Hz, 2H, phenyl-C$_{2,6}$-H); 8.46 (s, 1H, pyrazole-C$_5$-H); 8.79 (s, 1H, N=CH); 11.94 (s, 1H, NH, D$_2$O exchangeable). Elemental analysis Calcd for $C_{22}H_{21}N_9O_3S$ (491.53): C, 53.76; H, 4.31; N, 25.65; S, 6.52. Found: C, 53.85; H, 4.37; N, 25.93; S, 6.61.

3.1.4.2. 7-Ethyl-1,3-dimethyl-8-{4-{[(4-oxo-3-phenylthiazolidin-2-ylidene) hydrazono] methyl}-3-phenyl-1H-pyrazol-1-yl}-1H-purine-2,6(3H,7H)-dione ***(8b)***. Yield 80%, m.p 296–298 °C. IR (KBr, cm^{-1}): 1706 (br. C=O thiazolidinone and purine); 1660 (C=O purine); 1615 (C=N); 1291, 1033 (C–S–C). ^{1}H NMR (300 MHz, DMSO-d_6, δ ppm): 1.44 (t, J = 6.9 Hz, 3H, CH$_2$C$\underline{H}_3$); 3.26 (s, 3H, purine-N$_3$-CH$_3$); 3.45 (s, 3H, purine-N$_1$-CH$_3$); 4.1 (s, 2H, thiazolidinone-C$_5$-H); 4.64 (q, J = 6.9 Hz, 2H, C$\underline{H}_2$CH$_3$); 7.36 (d, J = 7.2 Hz, 2H, N-phenyl-C$_{2,6}$-H); 7.43–7.54 (m, 6H, phenyl- C$_{3,4,5}$-H and N-phenyl-C$_{3,4,5}$-H); 7.86 (dd, J = 7.5, 1.8 Hz, 2H, phenyl-C$_{2,6}$-H); 8.34 (s, 1H, pyrazole-C$_5$-H); 8.77 (s, 1H, N=CH). Elemental analysis Calcd for $C_{28}H_{25}N_9O_3S$ (567.62): C, 59.25; H, 4.44; N, 22.21; S, 5.65. Found: C, 59.38; H, 4.51; N, 22.34; S, 5.72.

3.1.4.3. 8-{3-(4-Chlorophenyl)-4-{[(4-oxothiazolidin-2-ylidene) hydrazono]methyl}-1H-pyrazol-1-yl}-7-ethyl-1,3-dimethyl-1H-purine-2,6(3H,7H)-dione ***(8c)***. Yield 83%, m.p > 300 °C. IR (KBr, cm^{-1}): 3135 (NH); 1706 (br. C=O thiazolidinone and purine); 1663 (C=O purine); 1640 (C=N); 1294, 1036 (C–S–C); 749 (C-Cl). ^{1}H NMR (300 MHz, DMSO-d_6, δ ppm): 1.46 (t, J = 6.5 Hz, 3H, CH$_2$C$\underline{H}_3$); 3.27 (s, 3H, purine-N$_3$-CH$_3$); 3.46 (s, 3H, purine-N$_1$-CH$_3$); 3.91 (s, 2H, thiazolidinone-C$_5$-H); 4.66 (q, J = 6.5 Hz, 2H, C$\underline{H}_2$CH$_3$); 7.57 (d, J = 8.4 Hz, 2H, 4-chlorophenyl-C$_{2,6}$-H); 7.98 (d, J = 8.4 Hz, 2H, 4-chlorophenyl-C$_{3,5}$-H); 8.50 (s, 1H, pyrazole C$_5$-H); 8.84 (s, 1H, N=CH); 11.91 (s, 1H, NH, D$_2$O exchangeable). Elemental analysis Calcd for $C_{22}H_{20}ClN_9O_3S$ (525.97): C, 50.24; H, 3.83; N, 23.97; S, 6.10. Found: C, 50.48; H, 3.81; N, 24.15; S, 6.23.

3.1.4.4. 8-{3-(4-Chlorophenyl)-4-{[(4-oxo-3-phenylthiazolidin-2-ylidene) hydrazono]methyl}-1H-pyrazol-1-yl}-7-ethyl-1,3-dimethyl-1H-purine-2,6(3H,7H)-dione ***(8d)***. Yield 98%, m.p > 300 °C. IR (KBr, cm^{-1}): 1707 (br. C=O thiazolidinone and purine); 1663 (C=O purine); 1615 (C=N); 1241, 1034 (C–S–C); 751(C-Cl). ^{1}H NMR (500 MHz, DMSO-d_6, δ ppm): 1.53 (t, J = 7.0 Hz, 3H, CH$_2$C$\underline{H}_3$); 3.44 (s, 3H, purine-N$_3$-CH$_3$); 3.61 (s, 3H, purine-N$_1$-CH$_3$); 3.97 (s, 2H, thiazolidinone-C$_5$-H); 4.86 (q, J = 7.0 Hz, 2H, C$\underline{H}_2$CH$_3$); 7.35 (d, J = 7.7 Hz, 2H, phenyl-C$_{2,6}$-H); 7.42–7.47 (m, 3H, 4-chlorophenyl-C$_{2,6}$-H and phenyl-C$_4$-H); 7.52 (t, J = 7.7 Hz, 2H, phenyl-C$_{3,5}$-H); 7.66 (d, J = 8.4 Hz, 2H, 4-chlorophenyl-C$_{3,5}$-H); 8.35 (s, 1H, pyrazole-C$_5$-H); 8.70 (s, 1H, N=CH). Elemental analysis Calcd for $C_{28}H_{24}ClN_9O_3S$ (602.07): C, 55.86; H, 4.02; N, 20.94; S, 5.33. Found: C, 56.08; H, 3.98; N, 21.18; S, 5.39.

3.1.4.5. 7-Ethyl-1,3-dimethyl-8-{4-{[(4-oxothiazolidin-2-ylidene) hydrazono]methyl}-3-(4-methyl- phenyl)-1H-pyrazol-1-yl}-1H-purine-2,6(3H,7H)-dione ***(8e)***. Yield 93%, m.p > 300 °C. IR (KBr, cm^{-1}): 3442 (NH); 1703 (br. C=O thiazolidinone and purine); 1666 (C=O purine); 1636 (C=N); 1242, 1034 (C–S–C). ^{1}H NMR (500 MHz, DMSO-d_6, δ ppm): 1.42 (t, J = 6.7 Hz, 3H, CH$_2$C$\underline{H}_3$); 2.34 (s, 3H, 4-methylphenyl-CH$_3$); 3.23 (s, 3H, purine-N$_3$-CH$_3$); 3.42 (s, 3H, purine-N$_1$-CH$_3$); 3.87 (s, 2H, thiazolidinone-C$_5$-H); 4.63 (q, J = 6.7 Hz, 2H, C$\underline{H}_2$CH$_3$); 7.30 (d, J = 8.0 Hz, 2H, 4-methylphenyl-C$_{3,5}$-H); 7.76 (d, J = 8.0 Hz, 2H, 4-methylphenyl-C$_{2,6}$-H); 8.44 (s, 1H, pyrazole- C$_5$-H); 8.75 (s, 1H, N=CH); 11.91 (s, 1H, NH, D$_2$O exchangeable). Elemental analysis Calcd for $C_{23}H_{23}N_9O_3S$ (505.55): C, 54.64; H, 4.59; N, 24.94; S, 6.34. Found: C, 54.91; H, 4.66; N, 25.23; S, 6.38.

3.1.4.6. 7-Ethyl-1,3-dimethyl-8-{4-{[(4-oxo-3-phenylthiazolidin-2-ylidene)hydrazono] methyl}-3-(4-methylphenyl)-1H-pyrazol-1-yl}-1H-purine-2,6(3H,7H)-dione ***(8f)***. Yield 84%, m.p 293–295 °C. IR (KBr, cm^{-1}): 1706 (br. C=O thiazolidinone and purine); 1662 (C=O purine); 1613 (C=N); 1239, 1033 (C–S–C). ^{1}H NMR (500 MHz, DMSO-d_6, δ ppm): 1.53 (t, J = 6.9 Hz, 3H, CH$_2$C$\underline{H}_3$); 2.40 (s, 3H, 4-methylphenyl-CH$_3$); 3.44 (s, 3H, purine-N$_3$-CH$_3$); 3.62 (s, 3H, purine-N$_1$-CH$_3$); 3.98 (s, 2H, thiazolidinone-C$_5$-H); 4.88 (q, J = 6.9 Hz, 2H, C$\underline{H}_2$CH$_3$); 7.32–7.57 (m, 9H, 4-methylphenyl-C$_{2,3,5,6}$-H and phenyl-C$_{2-6}$-H); 8.39 (s, 1H, pyrazole-C$_5$-H); 8.75 (s, 1H, N=CH). Elemental analysis Calcd for $C_{29}H_{27}N_9O_3S$ (581.65): C, 59.88; H, 4.68; N, 21.67; S, 5.51. Found: C, 60.03; H, 4.76; N, 21.82; S, 5.57.

3.1.4.7. 7-Ethyl-8-{3-(4-methoxyphenyl)-4-{[(4-oxothiazolidin-2-ylidene) hydrazono]methyl}-1H-pyrazol-1-yl}-1,3-dimethyl-1H-purine-2,6(3H,7H)-dione ***(8g)***. Yield 88%, m.p 296 decomp.°C. IR (KBr, cm^{-1}): 3439 (NH); 1704 (br. C=O thiazolidinone and purine); 1665 (C=O purine); 1635 (C=N); 1244 (C–O–C); 1029 (C–S–C). ^{1}H NMR (300 MHz, DMSO-d_6, δ ppm): 1.44 (t, J = 6.8 Hz, 3H, CH$_2$C$\underline{H}_3$); 3.25 (s, 3H, purine-N$_3$-CH$_3$); 3.42 (s, 3H, purine-N$_1$-CH$_3$); 3.81 (s, 3H, OCH$_3$); 3.89 (s, 2H, thiazolidinone- C$_5$-H); 4.64 (q, J = 6.8 Hz, 2H, C$\underline{H}_2$CH$_3$); 7.04 (d, J = 8.7 Hz, 2H, 4-methoxyphenyl-C$_{3,5}$-H); 7.82 (d, J = 8.7 Hz, 2H, 4-methoxyphenyl-C$_{2,6}$-H); 8.43 (s, 1H, pyrazole-C$_5$-H); 8.71(s, 1H, N=CH); 12.0 (s, 1H, NH, D$_2$O exchangeable). Elemental analysis Calcd for $C_{23}H_{23}N_9O_4S$ (521.55): C, 52.97; H, 4.44; N, 24.17; S, 6.15. Found: C, 53.18; H, 4.49; N, 24.51; S, 6.23.

3.1.4.8. 7-Ethyl-8-{3-(4-methoxyphenyl)-4-{[(4-oxo-3-phenylthiazolidin-2-ylidene)hydrazono]- methyl}-1H-pyrazol-1-yl}-1,3-dimethyl-1H-purine-2,6(3H,7H)-dione ***(8h)***. Yield 93%, m.p 291–293 °C. IR (KBr, cm^{-1}): 1704 (br. C=O thiazolidinone and purine); 1660 (C=O purine); 1610 (C=N); 1246 (C–O–C); 1030 (C–S–C). ^{1}H NMR (300 MHz, DMSO-d_6, δ ppm): 1.44 (t, J = 7.1 Hz, 3H, CH$_2$C$\underline{H}_3$); 3.26 (s, 3H, purine-N$_3$-CH$_3$); 3.44 (s, 3H, purine-N$_1$-CH$_3$); 3.81 (s, 3H, OCH$_3$); 4.11 (s, 2H,

thiazolidinone-C_5-H); 4.65 (q, J = 7.1 Hz, 2H, $C\underline{H}_2CH_3$); 7.05 (d, J = 8.7 Hz, 2H, 4-methoxyphenyl-$C_{3,5}$-H); 7.37 (d, J = 6.6 Hz, 2H, phenyl-$C_{2,6}$-H); 7.45–7.58 (m, 3H, phenyl-$C_{3,4,5}$-H); 7.83 (d, J = 8.7 Hz, 2H, 4-methoxyphenyl-$C_{2,6}$-H); 8.34 (s, 1H, pyrazole-C_5-H); 8.73 (s, 1H, N=CH). Elemental analysis Calcd for $C_{29}H_{27}N_9O_4S$ (597.65): C, 58.28; H, 4.55; N, 21.09; S, 5.37. Found: C, 58.53; H, 4.61; N, 21.37; S, 5.40.

3.2. Biological screening

3.2.1. In vitro 15-LOX inhibitory assay

Eighteen compounds were evaluated *in vitro* for their ability to inhibit 5-lipoxygenase enzyme. This was carried out using Abnova 15-lipoxygenase inhibitor screening assay kit (catalog no. KA1329, Cayman Chemicals), according to the manufacturer's instructions. Meclofenamate sodium, Quercetin and Zileuton were used as reference standards in the study. Solution of the test compounds in DMSO (10 µl) was added to the assay before initiating with substrate. Three concentrations were used (25, 50 and 100 µM) and the concentration that exert 50% enzyme inhibition was calculated according to manufacturer instructions [40].

Procedure:

- Blank Wells – add assay buffer (100 µl) to at least two wells.
- 15-LOX Standard wells add 15-LOX (90 µl) and assay buffer (10 µl) to at least two wells.
- 100% Initial activity wells – add LOX enzyme (90 µl) and DMSO (10 µl) to two wells. The 100% initial activity wells should produce approximately 10 nmol/min/ml of activity.
- Inhibitor Wells – add LOX enzyme (90 µl) and inhibitor (10 µl) to two wells.
- Add the substrate (linoleic acid, 10 µl) to all wells which will initiate the reaction. Shake the 96-well plate for at least 5 min.
- Add chromogen (100 µl) to each well to inhibit enzyme catalysis and develop the reaction. Cover with a plate cover and shake the 96-well plate for 5 min.
- The absorbance was read at 490–500 nm using a plate reader. For an accurate determination of reaction rates and IC_{50} values, samples were read kinetically, initial rate determination was based on the linear portion of the kinetic curve. The calculations were carried out in the following manner:
- Determine the average absorbance of all samples.
- Subtract the absorbance of background wells from absorbance of the 100% initial activity and the test compound wells.
- Percent inhibition = (100% Initial activity-test compound wells/100% Initial activity) × 100.
- Percent inhibition was graphed against inhibitor concentration to determine the IC_{50} value for each inhibitor.

3.2.2. Anticancer screening

The newly synthesized compounds were screened for their potential anticancer activity against five human cancer cell lines, A549 (lung), Caco-2 (colon), PC3 (prostate), MCF-7 (breast) and HepG-2 (liver) cancer cell lines using 5-FU as a standard anticancer drug by using MTT assay, described by Mosmann [36]. The A549, Caco-2 and PC3 cancer cells were routinely maintained as adherent cell cultures in DMEM containing 10% FBS and 2 mM L-glutamine, whereas MCF-7 and HepG-2 cancer cells were maintained as adherent cell cultures in RPMI 1640 media supplemented with 10% FBS and 2 mM L-glutamine at 37 °C in a humidified air incubator containing 5% CO_2. Cells were subcultured for two weeks before assay. Cell viability was assessed using trypan blue exclusion method. The anticancer assay involved three main steps. Firstly, the cancer cell suspension was prepared, then cancer cells were incubated with the tested compounds and finally, the inhibition of the growth rate of tumor cells was measured using the MTT assay. Cell suspension was inoculated into sterile 96-well flat-bottomed microtiter plates (3×10^3 cells/well for Caco-2, MCF-7 and HepG2 cell lines and 6×10^3 cells/well for A549 and PC3 cell lines). After cell attachment for 24 h, media were replaced with fresh culture media (blank wells) and media containing five concentrations (6.25, 12.5, 25, 50 and 100 µM) for each tested compound (compounds wells) or 5-FU (control wells). The plates were then incubated at 37 °C in 5% CO_2 incubator for 72 h. After incubation, MTT solution was added and the previously described method was applied. The percentage growth inhibition of tumor cells for every concentration of each tested compound was calculated according to the following formula:

$$\text{The growth inhibition } (\%) = 100 - \left[\frac{A_t\text{-}A_b}{A_c\text{-}A_b}\right]\text{x}100$$

Where: A_t: Absorbance of test compound.
A_b: Absorbance of blank.
A_c: Absorbance of control.

The effective anticancer activity of the tested compounds was evaluated by calculating the IC_{50} value which is the concentration of the drug causing 50% cell death (or 50% cytotoxicity) which was determined by Graphpad Instat 3.0 software using data obtained from the equation of the percentage growth inhibition. The results of the *in vitro* anticancer screening are listed in Table 2.

3.2.3. Antioxidant screening

3.2.3.1. Determination of the free radical scavenging activity by the 1,1-diphenyl-2-picrylhydrazyl (DPPH) antioxidant screening assay method. For each of the investigated compounds as well as the reference standard ascorbic acid (positive control) 10 µl of different concentrations (0.312, 0.625, 1.25, 2.5 and 5 µg/ml) solution in methanol were pipetted into a 96-well flat-bottomed plate, then, 100 µl of DPPH solution in methanol (0.004%) was added to each well. The plate was shaken to ensure thorough mixing and incubated protected from light at 25 °C for 30 min. The absorbance of the solution was measured at 517 nm. Methanol was used as a blank. The DPPH radical scavenging activity was calculated from the following equation:

$$\text{Percentage of radical scavenging activity} = [(A_b - A_t)/A_b] \times 100$$

Where:
A_b: Absorbance of blank
A_t: Absorbance of the tested compound or ascorbic acid

The antioxidant activity of the tested compounds (Table 3) was expressed as IC_{50} and determined by the Graphpad Instat 3.0 software using data calculated from the equation of percentage scavenging activity. The IC_{50} value was defined as the concentration (µg/ml) that inhibits the formation of DPPH radicals by 50% [41].

3.2.3.2. Determination of nitric oxide radical scavenging activity. This method consisted of the addition of 50 µl of the same serial concentrations of tested compounds, ascorbic acid (reference) or distilled water (as negative control) with 50 µl of sodium nitroprusside (10 mM) solution in water into a 96-well flat bottomed plate and the plate was incubated under light at RT for 90 min. Finally, an equal volume of Griess reagent (1% of sulfanilamide and 0.1% of naphthylethylenediamine in 2.5% H_3PO_4) was added to each well and the absorbance at λ = 490 nm was measured immediately. The NO radical scavenging activity was calculated from the following equation:

$$\text{Percentage of NO scavenging activity} = [(A_b - A_t)/A_b] \times 100$$

Where:
A_b: The absorbance of blank.
A_t: The absorbance of tested compound or ascorbic acid.

The antioxidant activity of the tested compounds (Table 4) was expressed as IC_{50} and determined by the Graphpad Instat 3.0 software using data calculated from the equation of percentage scavenging activity. The IC_{50} value was defined as the concentration (μg/ml) that inhibits the formation of NO radicals by 50% [38].

3.3. Molecular docking studies

The docking studies of compounds **4a, 7b, 7d, 7h, 8b** and **8d** were performed using Molecular operating environment (MOE 2016.0802) software (Chemical Computing Group, Montreal, Canada) [42].

The *in vitro* anticancer and antioxidant screening along with 15-lipoxygenase (15-LOX) inhibitory assay of the aforementioned compounds encouraged the molecular docking studies to help postulate the possible intermolecular interactions.

Crystal structure of 15-lipoxygenase was obtained from the protein data bank (PDB ID code: 1LOX, with the inhibitor RS7 bound in the active site). The targeted compounds were prepared by addition of hydrogens, calculation of the partial charges and energy minimization (using Force Field MMFF94X).

In addition, the protein structure was prepared by deleting water molecules and iron followed by addition of hydrogens and calculation of partial charges. Employment of the default protocol in MOE Dock application helped to find the favorable binding conformations of the test compounds, where triangle matcher and London dG were used as the placement method and the main scoring function, respectively. GBVI/WSA dG scoring function was applied as an additional refinement step using rigid receptor method.

The output database comprised the energy scores in kcal/mol for the complexes formed between the ligand conformers and the binding sites. Ultimately, the produced docking poses were studied and the different interactions with the active site residues were analyzed.

4. Conclusion

The principal aim of this study was to synthesize and investigate the 15-LOX inhibitory activities, anticancer, and anti-oxidant potential of some new purine/pyrazole hybrids with the hope of discovering new lead structures devoid of toxic effects associated with conventional anticancer agents. Additionally, molecular docking studies were performed in order to investigate the possible binding mode of the most active compounds with the active site of 15-LOX enzyme. The obtained results clearly revealed that compounds **4a**, **4b**, **5a**, **6b**, **7b**, **7d**, **7h**, **8b**, **8d** and **8h** (IC_{50} range 1.76–2.64 μM) showed potential 15-LOX inhibition activity at concentration lower than that of the standard inhibitors quercetin, meclofenamate sodium and zileuton. Compounds **4a, 7d, 7h** and **8d** were the most potent (IC_{50} = 1.76–1.98 μM) that gave potency 2 times that of zileuton and about 3 times that of quercetin and meclofenamate sodium. In addition, the anticancer activity testing revealed that compound **7b** and **8b** displayed broad spectrum anticancer activity. Whereas, compound **7h** demonstrated moderate anticancer activity against lung A549 and colon Caco-2 cell lines. Moreover, compound **8b** can be considered as the best DPPH scavenger among the tested compounds. In addition, compounds **5a, 5b, 6b** and **7b, 7h** exhibited good DPPH free radical scavenging potential with IC_{50} ranging from 4.89 to 14.43 μg/ml higher than that of the standard ascorbic acid with IC_{50} value of 15.34 μg/ml. Furthermore, compounds **4d, 5a, 5b** and **7b** exerted potent NO scavenging ability. Molecular docking study of **4a**, **7b**, **7d**, **7h**, **8b** and **8d** showed nearly the same binding pattern as that of **RS7** within 15-LOX active site, where the presence of either rhodanine moiety or thiazolidinone ring together with the purine scaffold ensured high recognition within the enzyme's active site. Consequently, compounds **7b, 7h** and **8b** are considered promising 15-LOX inhibitors with anti-cancer and antioxidant potential that promotes more investigation and derivatization

References

[1] F.Q. Shen, Z.C. Wang, S.Y. Wu, S.Z. Ren, R.J. Man, B.Z. Wang, H.L. Zhu, Bioorg. med. Chem. Let. 27 (2017) 3653–3660.
[2] D. Kerjaschki, J. Clin. Investig. 121 (2011) 2000–2012.
[3] A. Orafaie, M.M. Matin, H. Sadeghian, Cancer Metastasis Rev. 37 (2018) 397–408.
[4] U.P. Kelavkar, J.B. Nixon, C. Cohen, et al., Carcinogenesis 22 (2001) 1765–1773.
[5] H. Sadeghian, A. Jabbari, Expert Opin. Ther. Patents 26 (1) (2016) 65–88.
[6] H.A. Abd El Razik, M. Mroueh, W.H. Faour, W.N. Shebaby, C.F. Daher, H.M.A. Ashour, H.M. Ragab, Chem. Biol. Drug Des. 90 (2017) 83–96.
[7] B. Poeggeler, M.A. Pappolla, R. Hardeland, A. Rassoulpour, P.S. Hodgkins, P. Guidetti, R. Schwarcz, Brain Res. 815 (2) (1999) 382–388.
[8] B.T. Moorthy, S. Ravi, M. Srivastava, K.K. Chiruvella, H. Hemlal, O. Joy, S.C. Raghavan, Bioorg. Med. Chem. Lett. 20 (2010) 6297–6301.
[9] P.J. O'Dwyer, D.D. Shoemaker, H.N. Jayaram, D.G. Johns, D.A. Cooney, S. Marsoni, L. Malspeis, J. Plowman, J.P. Davignon, R.D. Davis, Invest. New. Drug. 2 (1984) 79–84.
[10] K.S. Sharath Kumar, A. Hanumappa, M. Vetrivel, M. Hegde, Y.R. Girish, T.R. Byregowda, S. Rao, S.C. Raghavan, K.S. Rangappa, Bioorg. Med. Chem. Lett. 25 (17) (2015) 3616–3620.
[11] V. Jaishree, N. Ramdas, J. Sachin, B. Ramesh, J. Saudi. Chem. Soc. 16 (4) (2012) 371–376.
[12] B. Šarkanj, M. Molnar, M. Čačić, L. Gille, Food Chem. 139 (1–4) (2013) 488–495.
[13] R. Revathi, D.A. Ananth, T. Sivasudha, P.S. Elizabeth, Adv. Sci. focus 2 (2014) 1–8.
[14] E. Abdelall, G. Kamel, Eur. J. Med. Chem. 118 (2016) 250–258.
[15] S. Sharma, S. Mehndiratta, S. Kumar, J. Singh, P.M.S. Bedi, K. Nepali, Recent Pat. Anticancer Drug Discov. 10 (3) (2015) 308–341.
[16] F.A. Ashour, S.M. Rida, S.A.M. El-Hawash, M.M. ElSemary, M.H. Badr, Med. Chem. Res. 21 (7) (2012) 1107–1119.
[17] L.P. Jordheim, D. Durantel, F. Zoulim, C. Dumontet, Nat. Rev. Drug Discov. 12 (6) (2013) 447–464.
[18] M. Zygmunt, G. Chłoń-Rzepa, J. Sapa, Pharmacol. Rep. 66 (6) (2014) 996–1100.
[19] S.B. Wang, P. Jin, F.N. Li, Z.S. Quan, Eur. J. Med. Chem. 84 (2014) 574–583.
[20] O. Baszczyński, D. Hocková, Z. Janeba, H. Antonín, J. Petr, Eur. J. Med. Chem. 67 (2013) 81–89.
[21] A.K.M. Hayallah, A.A. Talhouni, A.A.M. Abdel Alim, Arch. Pharm. Res. 35 (8) (2012) 1355–1368.
[22] A. Brathe, G. Andresen, L.L. Gundersen, K.E. Malterud, F. Rise, Bioorg. Med. Chem. 10 (2002) 1581–1586.
[23] P. Furet, J. Schoepfer, T. Radimerski, P. Chène, Bioorg. Med. Chem. Lett. 19 (15) (2009) 4014–4017.
[24] L. Llauger, H. He, J. Kim, J. Aguirre, N. Rosen, U. Peters, P. Davies, G. Chiosis, J. Med. Chem. 48 (2005) 2892–2905.
[25] R. Jorda, L. Havlicek, I.W. McNae, M.D. Walkinshaw, J. Voller, et al., J. Med. Chem. 54 (2011) 2980–2993.
[26] S. Blanchard, C.K. Soh, C.P. Lee, et al., Bioorg. Med. Chem. Lett. 22 (8) (2012) 2880–2884.
[27] P. Raboisson, C. Lugnier, C. Muller, et al., Eur. J. Med. Chem. 38 (2003) 199–214.
[28] C.Y. Hsu, C.H. Lin, J.T. Lin, Y.F. Cheng, H.M. Chen, S.H. Kao, Mol. Med. Rep. 12 (2015) 4566–4571.
[29] M.A.N. Mosselhi, M.A. Abdallah, N.H. Metwally, I.A. El-Desoky, L.M. Break, ARKIVOC 14 (2009) 53–63.
[30] O.G. Shaaban, H.A. Abd El Razik, S.A. Shams El-Dine, F.A. Ashour, A.A. El-Tombary, O.S. Afifi, M.M. Abu-Serie, Future Med. Chem. 10 (12) (2018) 1449–1464.
[31] X. Li-Li, Z. Chang-Ji, S. Liang-Peng, M. Jing, P. Hu-Ri, Eur. J. Med. Chem. 48 (2012) 174–178.
[32] M.X. Song, C.J. Zheng, X.Q. Deng, L.P. Sun, Y. Wu, L. Hong, Y.J. Li, Y. Liu, Z.Y. Wei, M.J. Jin, H.R. Piao, Eur. J. Med. Chem. 60 (2013) 376–385.
[33] M. Azizmohammadi, M. Khoobi, A. Ramazani, S. Emami, A. Zarrin, O. Firuzi, R. Miri, A. Shafiee, Eur. J. Med. Chem. 59 (2013) 15–22.
[34] A.A. Bekhit, A.M.M. Hassan, H.A. Abd El Razik, M.M.M. El-Miligy, E.J. El-Agroudy, A.E.-D.A. Bekhit, Eur. J. Med. Chem. 94 (2015) 30–44.
[35] H.S. Elbordini, M.M. El-Miligy, S.E. Kassab, H. Daabees, W.A.M. Ali, S.A.M. El-Hawash, J. Med. Chem. 10 (145) (2018) 594–605.
[36] T. Mosmann, J. Immunol. Methods 65 (1) (1983) 55–63.
[37] A. Braca, N. De Tommasi, L.D. Bari, C. Pizza, M. Politi, I. Morelli, J. Nat. Prod. 64 (7) (2001) 892–895.
[38] S.C. Ho, Y.L. Tang, S.M. Lin, Y.F. Liew, Food Chem. 119 (3) (2010) 1102–1107.
[39] K.E. Hevener, W. Zhao, D.M. Ball, K. Babaoglu, J. Qi, S.W. White, R.E. Lee, J. Chem. Inf. Model. 49 (2) (2009) 444–460.
[40] P. Plackova, M. Sala, M. Smidkova, M. Dejmek, H. Hrebabecky, R. Nencka, H.J. Thibaut, J. Neyts, H. Mertlikova-Kaiserova, Free Radical Biol. Med. 97 (2016) 223–235.
[41] N. Gherraf, S. Ladjel, B. Labed, S. Hameuralaine, Plant Sci. Feed 1 (9) (2011) 155–159.
[42] Molecular Operating Environment (MOE). < https://www.chemcomp.com > .